ORNL/TM-2015/23

Cadmium Subtraction Method for the Active Albedo Neutron Interrogation of Uranium

Louise G. Worrall
Stephen Croft

February 2015

OAK RIDGE NATIONAL LABORATORY
MANAGED BY UT-BATTELLE FOR THE US DEPARTMENT OF ENERGY

ORNL/TM-2015/23

Nuclear Security and Isotope Technology Division

CADMIUM SUBTRACTION METHOD FOR THE ACTIVE ALBEDO NEUTRON INTERROGATION OF URANIUM

Louise G. Worrall and Stephen Croft

Date Published: February 2015

Prepared by
OAK RIDGE NATIONAL LABORATORY
Oak Ridge, Tennessee 37831-6283
managed by
UT-BATTELLE, LLC
for the
US DEPARTMENT OF ENERGY
under contract DE-AC05-00OR22725

CONTENTS

Page

LIST OF FIGURES

LIST OF TABLES

Table **Page**

ACRONYMS

AANI	Active Albedo Neutron Interrogation
AWCC	Active Well Coincidence Counter
BIC	Burnup, Initial Enrichment, and Cooling Time
CIPN	Californium-252 Interrogation with Prompt Neutron Detection
DDSI	Differential Die-away Self-Interrogation
DMM	Direct Multiplication Measurement
HDPE	High-Density Polyethylene
HV	High Voltage
IAEA	International Atomic Energy Agency
INCC	IAEA Neutron Coincidence Counting Software
JSR	Jomar Shift Register (Manufactured by Canberra Industries, Inc.)
LAWCC	Large Volume Active Well Coincidence Counter
LEU	Low Enriched Uranium
MDA	Minimum Detectable Activity
MSR	Multiplicity Shift Register
NBL	New Brunswick Laboratory
NBS	National Bureau of Standards
NDA	Nondestructive Assay
NGSI	Next Generation Safeguards Initiative
NIST	National Institute of Standards and Technology
ORNL	Oak Ridge National Laboratory
PNAR	Passive Neutron Albedo Reactivity
PNAR-^{3}He	Passive Neutron Albedo Reactivity with ^{3}He Tubes
PNAR-FC	Passive Neutron Albedo Reactivity with Fission Chambers
PNEM	Passive Neutron Enrichment Meter
PSMC	Passive Neutron Multiplicity Counter
PWR	Pressurized Water Reactor
SF	Spontaneous Fission
SNF	Spent Nuclear Fuel
SNM	Special Nuclear Material

ACKNOWLEDGMENTS

The authors would like to acknowledge and thank the US Department of Energy (DOE) National Nuclear Administration (NNSA), Office of Nonproliferation and Arms Control (NPAC) and the Next Generation Safeguards Initiative (NGSI) for providing funding for this work.

The authors would also like to acknowledge and thank the extended Oak Ridge National Laboratory team:

Jason D. Braden
Steven L. Cleveland
Ian G. Gross
Robert D. McElroy, Jr.

EXECUTIVE SUMMARY

This report describes work performed under the Next Generation Safeguards Initiative (NGSI) Cadmium Subtraction Project. The project objective was to explore the difference between the traditional cadmium (Cd) ratio signature [1] and a proposed alternative Cd subtraction (or Cd difference) approach. The thinking behind the project was that a Cd subtraction method would provide a more direct measure of multiplication than the existing Cd ratio method. At the same time, it would be relatively insensitive to changes in neutron detection efficiency when properly calibrated. This is the first published experimental comparison and evaluation of the Cd ratio and Cd subtraction methods.

In this project, an experimental measurement campaign was performed at Oak Ridge National Laboratory (ORNL) using the Large Active Well Coincidence Counter (LAWCC) in a new mode. A simple adaption of the existing counter design was made using a ^{252}Cf spontaneous fission neutron source and an insert of high-density polyethylene (HDPE) and Cd. This enabled the counter to be used for the active albedo neutron interrogation (AANI) of small uranium-bearing items (up to 194 g total U was available). The insert was designed to create a re-entrant neutron flux (thermal neutron albedo) in the condition without Cd. Cadmium was then used to absorb the slow component of the re-entrant neutron flux to create a second measurement condition. The difference between the detected neutron events for these two measurement conditions corresponds to the additional neutron events from fission induced by the thermal neutron albedo. The ability to use the LAWCC in a new mode using AANI has the field implementation benefit of enabling a Cd subtraction calibration curve to be determined for uranium mass, without the use of AmLi sources and with a counter of modest efficiency, i.e., without having to use an instrument with greater ^{3}He requirements or an overly complex instrument. In the experimental configuration as applied, collected data can also be used as a future extension of the ORNL-developed Direct Multiplication Measurement (DMM) technique [2].

The Cadmium Subtraction Project has measured and evaluated the Cd subtraction and traditional Cd ratio signatures for a range of small uranium-bearing items. Both signatures showed a measurable effect and could be fit to a calibration curve for the assay of ^{235}U mass. However, there is no obvious merit of one method over the other with this data set because the signal, although measurable, was small. The small signal was due to low item multiplication ($M-1$ ~ few %) because of the low mass of fissile material.

The experimental measurement campaign has demonstrated that the coincidence gate fraction changes with time after a ^{252}Cf spontaneous fission event during a measurement with a re-entrant neutron flux, which causes the Cd subtraction or Cd ratio signature to vary as a function of time. These experimental findings illustrate that a reliance on traditional IAEA settings for coincidence counting (4.5 μs pre-delay and 64 μs gate width) and the procedures used to derive those settings should be challenged and reconsidered when the measurement objective is to derive signatures other than the doubles rate, especially when the counter time behavior is varying due to a re-entrant neutron flux. These findings emphasize the need for incremental research and development (R&D) for safeguards technology. NDA instruments themselves do not always have to be redesigned or completely reimagined to generate new methods or new signatures/observables, or indeed to optimize current signatures/observables. It is not always necessary to redesign new hardware or create transformational techniques to extract new signatures from current NDA methods and to yield new ways to observe fissile content. As this project has demonstrated, incremental R&D such as changing the coincidence gate settings, or delaying a coincidence gate in time, can vary and in turn improve the signature. Future work on signature optimization is recommended from a safeguards perspective, using kilogram quantities of uranium of safeguards relevance.

1. CADMIUM SUBTRACTION METHOD

Here, the history of neutron counting based on a re-entrant neutron flux (thermal neutron albedo), the thought process behind the project, and the safeguards relevance of the project are described. Simple theory and a functional form for the Cd subtraction algorithm are also presented.

1.1 HISTORY AND SAFEGUARDS TECHNOLOGY DEVELOPMENT CHALLENGE

Safeguards technologies based on the principle of a re-entrant neutron flux are being developed in the context of the Next Generation Safeguards Initiative (NGSI) Spent Nuclear Fuel Nondestructive Assay (NDA) project and other international collaborations, including UF_6 cylinder assay. Menlove and Beddingfield [1] were the first proponents of the method for safeguards neutron coincidence counting. Since then, the principle of a re-entrant neutron flux has been applied to safeguards neutron counting measurements, both total and correlated neutron counting, for two safeguards applications (spent nuclear fuel verification and UF_6 cylinder assay for mass and enrichment verification) and in three resulting safeguards technology NDA measurement systems supported by NGSI: Passive Neutron Albedo Reactivity with Fission Chambers (PNAR-FC) [3]; PNAR with ^{3}He gas-filled proportional counters (PNAR-^{3}He) (supported in the past but succeeded by Differential Die-away Self-Interrogation, or DDSI) [4,5]; and the Passive Neutron Enrichment Meter (PNEM) [6]. These techniques, with the exception of DDSI, all feature neutron measurements performed with and without Cd. Data analyses are based on the Cd ratio method, which is the ratio of the detector response without a Cd liner surrounding the assay item to the response with an item Cd liner present. The Cd ratio method has traditionally been applied to determine reactivity and, therefore, to infer fissile content in a measured item.

The safeguards technology development challenge posed by these techniques is extracting a signal from the assay results that is both measurable and meaningful, easily interpreted, and uniformly maps to the attribute of interest. The goal of correlated neutron counting using the Cd ratio is to separate the primary emission neutrons from the fission neutrons induced in the sample material. However, in the application of the Cd ratio method to date, several assumptions are made. It has been postulated that the standard Cd ratio analysis method makes an approximate and unqualified assumption regarding the exact cancellation of the albedo neutron source term. The assumption that the albedo neutron source term is equal in the case of the two measurement conditions (i.e., with and without Cd) and therefore, cancels out in the ratio, cannot be made because the neutron detection efficiency is different in the case of the two measurement conditions. The calculated result is, therefore, partly representative of detecting a small change in neutron detection efficiency and cannot be solely attributed to the intended change in multiplication.

Furthermore, the Cd ratio algorithm itself is not embedded within the IAEA Neutron Coincidence Counting (INCC) software, the IAEA use code, and is used on an ad hoc basis (e.g., in spreadsheets). Therefore, there is also an opportunity to implement a new method into the INCC software.

This report describes an alternative Cd subtraction method. This work differs in focus from other safeguards technology development efforts employing the standard Cd ratio method for Pu or UF_6 cylinder assay and is instead applied to the active neutron interrogation of uranium. In particular, this work is directed at fielding a replacement algorithm based on a Cd subtraction approach. Furthermore, this project extends the safeguards application of the method to the assay of small uranium-bearing items (up to 194 g total U).

The passive assay of bulk uranium is challenging because the principal gamma-rays are strongly self-absorbed and the neutron emissions are weak. Active neutron interrogation is, therefore, frequently the method of choice.

1.2 THOUGHT PROCESS: WHY A "CADMIUM SUBTRACTION" APPROACH?

The NDA technique of Active Albedo Neutron Interrogation (AANI) is based on the principle of a re-entrant neutron flux. The technique is "active" in the sense that a ^{252}Cf spontaneous fission neutron source is used as the primary interrogation source. Neutrons from the primary induced fission process are then moderated/reflected back in to the item, which results in the secondary interrogation source known as the "thermal" neutron albedo (note that thermal is being used as a convenience to mean slow neutrons below the Cd cut-off, but predominantly thermalized). Measurements are performed with and without Cd because Cd is used to absorb the slow component of the re-entrant neutron flux to create a second measurement condition. A thin (~1–2 mm) Cd sheet effectively removes all neutrons below about 0.4 eV from the returning flux. The difference between (or subtraction of) the detected neutron events for these two measurement conditions should correspond to the additional neutron events from fission induced by the thermal neutron albedo. Hence, a Cd subtraction approach is taken.

The diagram below is taken from prior simulation work for NGSI [4], but is referenced for illustration of the thought process. Figure 1 shows the average neutron population (total number of neutron captures) in the detection system following a single spontaneous fission event, which has the nature of a Rossi-Alpha distribution. In the case of spent nuclear fuel assay, which is illustrated in the figure, the driving interrogation source neutrons are born from ^{244}Cm spontaneous fission and the source is internal to the item under assay. While the primary interrogation source is inducing fission, some neutrons are detected directly from the source. As the die-away of neutrons from the primary interrogation source can be observed in the detector (^{244}Cm captures curve below), an increase in the population of neutron captures from induced fission events within the assay item can also be observed as an in-growth of the neutron population, which is delayed in time (as evidenced by the "total fissile" captures curve below). The underlying physics will be the same for our experiment. However, in the Cd subtraction experiment, the primary interrogation source is ^{252}Cf and it is external to the item. The source is also constant. The timescales (x-axis) will be different from the spent nuclear fuel application.

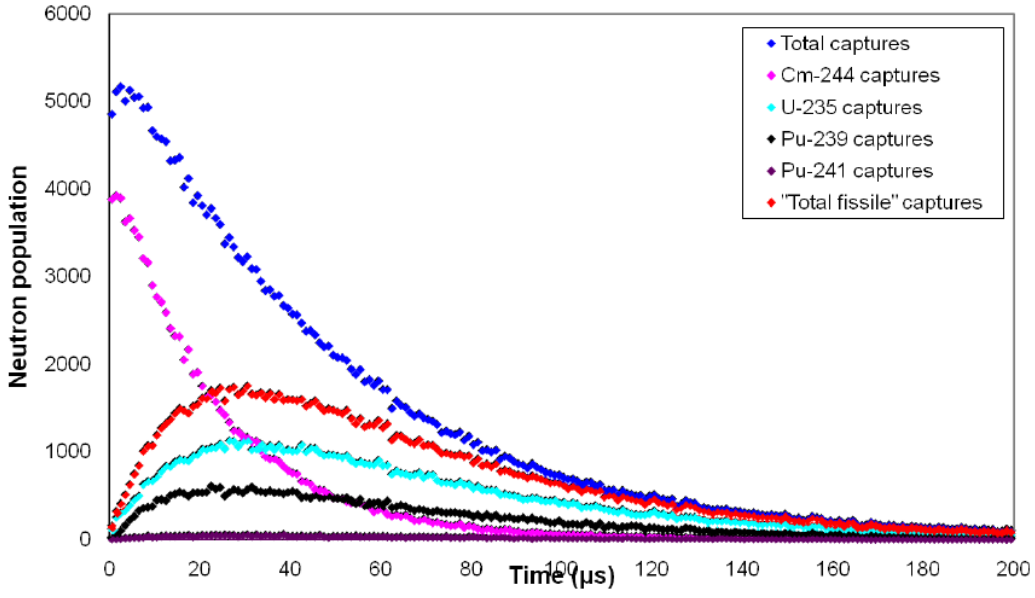

Fig. 1. Simulated time profile of the neutron population in a spent nuclear fuel neutron NDA system.

The measurement with the Cd liner should yield a detector response that is proportional to the fission rate in the item without reflection and is, therefore, indicative of the strength of the primary interrogation source. The measurement without the Cd liner should yield a detector response that is proportional to the albedo induced fission in the item with reflection (secondary emission, thermal fission). The Cd ratio was intended to provide the difference in multiplication only. However, the ratio is also sensitive to any change in detection efficiency. The neutron detection efficiency changes in the Cd and no Cd case because of the spatial-energy coupling between zones (i.e., item, reflector, cavity, and detector), even with the fixed Cd liner in place. Therefore, the Cd ratio does not provide an exact cancellation of the driving source term.

The Cadmium Subtraction Project set out to solve this challenge by providing measured data and corresponding analysis to demonstrate this change in neutron detection efficiency and further to determine whether a Cd difference or subtraction method yielded a direct observable of multiplication compared to the Cd ratio method. The objectives of the project were the following:

- Compare the Cd ratio and Cd subtraction methods empirically and determine which method provides the more direct measure of multiplication
- Develop a cadmium subtraction algorithm for use within in-field analysis tools such as INCC with active neutron interrogation parameters included in the algorithm
- Test the new developed algorithm against data collected using the LAWCC at ORNL, acquired with and without a Cd liner present
- Perform an active neutron measurement campaign using resources already available at ORNL

1.3 NDA SCIENCE

Fission has to be induced in fissile materials (odd mass number) due to their low specific rate of spontaneous fission. Neutron-induced fission can arise from active interrogation (with an external neutron source) or self-interrogation (with an internal neutron source, e.g., spontaneous fission). Therefore, there are currently two different categories of NDA techniques based on a returning or re-entrant neutron flux (albedo), and the Cd subtraction method could be applied in either case:

- **Albedo with internal neutron source** for items with a high internal spontaneous fission rate (e.g., self-interrogation with and without Cd, PNAR for SNF, PNEM for UF_6 cylinders)
- **Albedo with external neutron source** for items with a negligible internal spontaneous fission rate (e.g., active neutron interrogation with and without Cd, AANI using the LAWCC applied to the assay of small uranium-bearing items)

A step-by-step guide to the physics processes in the coupled item-counter system is described for both a self-interrogation experiment with an internal neutron source, and an active neutron experiment with an external neutron source is provided below. This leads in to the development of a functional form for the Cd subtraction method.

Albedo with external neutron source – LAWCC experiment

Without Item Cd Liner	***With Item Cd Liner***
1) External source neutrons being measured – initial neutron number (assuming negligible spontaneous fission and alpha in the item) 2) Transmission of the external source neutrons – gain of neutrons 3) Fission induced by the external source neutrons within the item – neutron gain via multiplication (first induced fission chain) 4) Emission of the primary induced fission neutrons via item leakage 5) Reflection of the external source neutrons 6) Reflection of the induced fission neutrons 7) Fission induced by the reflected neutrons – gain of neutrons via multiplication (second induced fission chain) 8) Emission of the secondary induced fission neutrons via item leakage 9) Ignore further reflections 10) Detection of the source neutrons 11) Detection of the fission neutrons (due to source) 12) Detection of the fission neutrons (due to reflection)	1) External source neutrons being measured – initial neutron number (*assuming negligible spontaneous fission and alpha in the item*) 2) Transmission of the external source neutrons – gain of neutrons 3) Fission induced by the external source neutrons within the item – neutron gain via multiplication (first induced fission chain) 4) Emission of the primary induced fission neutrons via item leakage 5) Absorption of the source neutrons in the Cd (thermal and epi-thermal component) 6) Absorption of the induced fission neutrons in the Cd (thermal and epi-thermal component) 7) Detection of the source neutrons 8) Detection of the fission neutrons (due to source) *Note: this is an over-simplification since the fast-neutron component can still be reflected and will not be absorbed by the Cd.*

Albedo with internal neutron source – spent nuclear fuel NDA

Without Item Cd Liner	***With Item Cd Liner***
1) Internal source neutrons being measured – initial neutron number 2) Emission of the internal source neutrons – loss of neutrons via item leakage 3) Fission induced by the internal source neutrons within the item – gain of neutrons via item multiplication (first induced fission chain) 4) Emission of the primary induced fission neutrons via item leakage 5) Reflection of the source neutrons 6) Reflection of the induced fission neutrons 7) Fission induced by the reflected neutrons – gain of neutrons via multiplication (second induced fission chain) 8) Emission of the secondary induced fission neutrons via item leakage 9) Ignore further reflections 10) Detection of the internal source neutrons 11) Detection of the fission neutrons (due to source) 12) Detection of the fission neutrons	1) Internal source neutrons being measured – initial neutron number 2) Emission of the internal source neutrons – loss of neutrons via item leakage 3) Fission induced by the internal source neutrons within the item – gain of neutrons via item multiplication (first induced fission chain) 4) Emission of the induced fission neutrons via item leakage 5) Absorption of the source neutrons in the Cd (thermal and epi-thermal component) 6) Absorption of the induced fission neutrons in the Cd (thermal and epi-thermal component) 7) Detection of the internal source neutrons 8) Detection of the induced fission neutrons (due to source) *Note: this is an over-simplification since the fast-neutron component can still be reflected and will not be absorbed by the Cd.*

1.4 THEORETICAL ALGORITHM DEVELOPMENT

The neutron reactivity of a multiplying item is a measure of the induced fission rate within an item and is often expressed by an effective multiplication factor, k_{eff}, or by a multiplication parameter, M, such as that used in the neutron point model equations embedded within neutron analysis tools such as INCC. The neutron reactivity of a multiplying item is not a fixed physical characteristic of the item, which may be used to uniquely describe the item. Instead, it is a property that is dependent on the environment in which the item is placed. This principle can be applied for criticality safety and is used when safely storing multiplying items in close proximity, such as when storing spent nuclear fuel assemblies in poisoned racks under boronated water. The idea of using passive (or self, from Pu spontaneous fission (SF), Cm SF or, e.g., F(α,n) depending on the circumstances) neutron interrogation, or an external neutron driver, together with a change in the environment as a means to determine information of safeguards significance about an object has been discussed for a number of years [1,3,4,5,7,8]. One of the simplest ways to change the environment is to insert a slow (thermal and epi-thermal) neutron absorber, such as Cd, to block returning neutrons degraded in energy.

Recently, Bolind [9] has developed an analytical theory of the PNAR-FC and ^{252}Cf Interrogation with Prompt Neutron Detection methods for underwater spent nuclear fuel (SNF) characterization in order to explain why they are closely allied approaches, in the sense that they both provide a measure of reactivity. They also share some key underlying dependence on the BIC parameters (burnup, initial enrichment, and cooling time), which provide a crude means to describe the isotopic composition of spent low-enriched uranium (LEU) pressurized water reactor (PWR) fuel assemblies. After carefully stating his simplifying assumptions and clearly describing his notation, Bolind's analysis is based on a simple neutron-balance (probability or bookkeeping), i.e., gross (one energy group) counting in the steady state. Practical challenges are not addressed; for instance, equivalence of counting efficiency is simply assumed (without considering the influence of the neutron energy spectrum on the neutron detection efficiency) and the variation of boron concentration is dismissed as a matter of calibration. The detailed properties of the measurement item are not considered. Put another way, the expressions obtained are in terms of model-specific parameters, and the interpretation (or inversion) of which is not considered.

By introducing albedo parameters to represent the probability of neutrons exchanging between the item and its environment, a detailed discussion is avoided on the complex geometrical and material-dependent neutron transport processes taking place. This includes the coupling of the item to its surroundings and the spatial and temporal properties of the returning thermal flux. But it also conceals all of the important functional dependences of the problem. Furthermore, the approach does not consider PNAR-^{3}He based on coincidence counting because additionally PNAR-^{3}He requires the time domain to be understood [4]. In that regard, the approach of Bolind [9] does not consider the doubles neutron counting rate signature and only considers the singles rate signature (time-averaged neutron balance).

To address the problem from first principles, even in a rudimentary way, requires at a minimum a two energy groups (fast and slow [thermal and epi-thermal]), three spatial zones (assay-item "multiplying core," coupled to the external and coupled reflector and detector), and time-dependent neutron transport treatment. This is the only way that a spatial and temporal distribution for the thermal interrogation flux emerges (e.g., peaking in the reflector)—behaviors that are distinct from the fast-neutron flux (or from a one-group approximation). With this level of complexity, the transport equation cannot be solved by separation of variables (as is the case for a simple one-group reflected core), nor is it any more analytically tractable. Furthermore, if a low-order multi-group approximation is to quantitatively capture the essence of the problem, the challenge of how to select the group constants is also faced. This forces the use of more sophisticated, exact, numerical methods such as Monte Carlo simulation [10], even for deeply sub-critical and isolated geometries [11, 12].

In the present work, experimental investigation is emphasized because feasibility also depends on establishing that there is a signature that can be measured with adequate precision, and current standard simulation methods (Monte Carlo N-Particle Extended, MCNPx, coincidence tally) do not predict precision directly. The accidental coincidence rate requires post-processing and is often ignored in design studies.

Having warned that simple models have limited predictive or interpretive value, the familiar point model expressions are used to raise a few significant points.

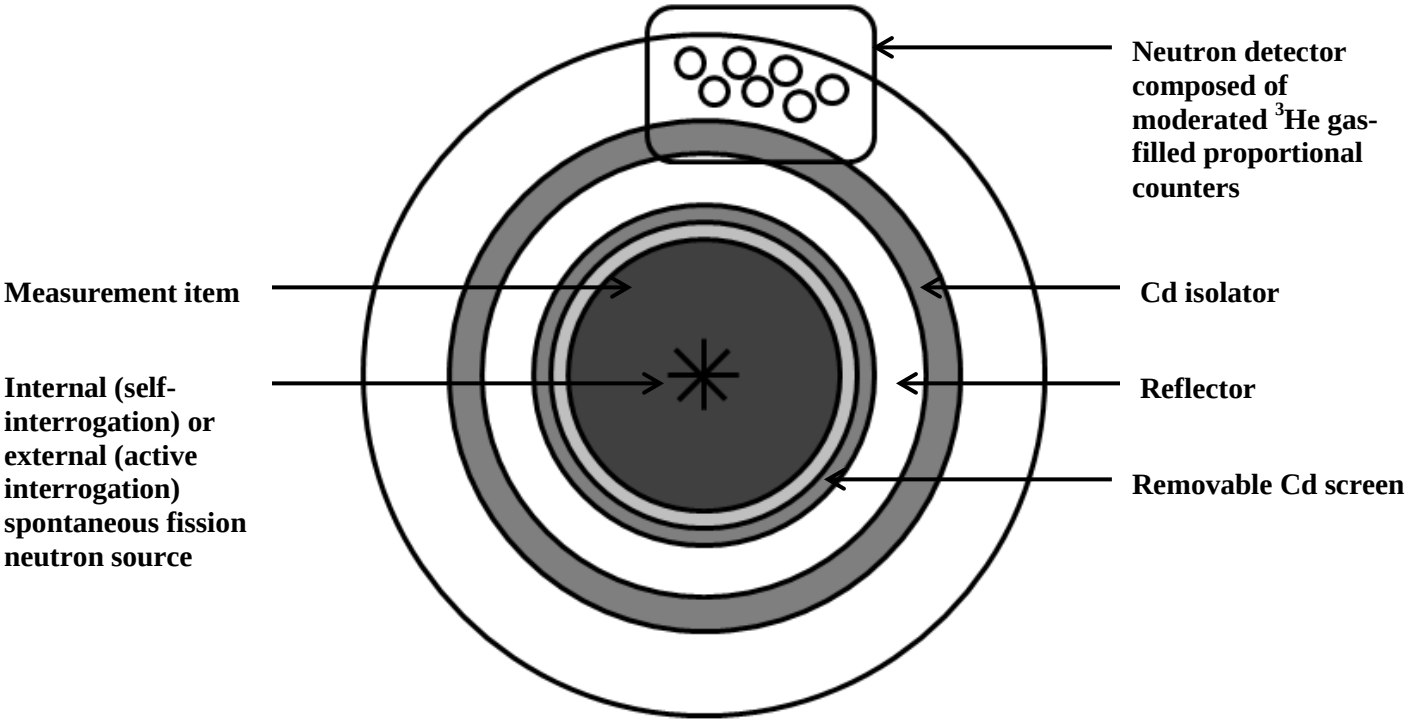

Fig. 2. Conceptual schematic diagram of the measurement configuration.

The conceptual arrangement of Fig. 2 is used for simplicity. The multiplying item is depicted as the core at the center of the assembly and is seen to contain the primary sources of neutrons (SF and (α,n), although these can be combined into a single composite random emitter with suitably chosen emission multiplicity distribution). Around the item is a moderating reflector. This reduces neutron leakage, flattens the flux profile inside the item, and elevates neutron production through induced fission. Outside the reflector we have an external detector to record the emergent neutron chains. Between the reflector and detector is a sheet of Cd. Consequently, the slow neutrons leaving the reflector are absorbed by the item Cd liner and are not detected. In addition, neutrons that have been moderated in the body of the counter cannot return to the item. Fast neutrons are only created in the measurement item (the core) either through the primary (passive) source term or by the action of induced fission by both fast and slow neutrons. The environment is changed by the insertion or removal of the Cd sheet located between the measurement item and the reflector. It can be imagined that the only influence of the Cd is the removal of slow neutrons, which would otherwise enter the item from the reflector. The point model expressions for singles (*S*) and doubles (*D*) are now documented for this measurement situation.

The fully (bias, deadtime, normalization, and background) corrected net *S* and *D* rates observed experimentally are related to the properties of the item and the neutron detector through algebraic relationships derived from the 1-energy group, prompt induced fission, point model [13,14]. One way to write these relations in compact form is as follows:

$$S = F_S.(\varepsilon.M_L).\left(\frac{\nu_{S1}}{1}\right).(1+\alpha) \quad (1)$$

$$D = F_S.(\varepsilon.M_L)^2.\left(\frac{\nu_{S2}}{2}\right).f_d.\left[1+\frac{(M_L-1)}{(\nu_{I1}-1)}.(1+\alpha).\frac{\nu_{S1}}{\nu_{S2}/2}.\frac{\nu_{I2}}{2}\right] \quad (2)$$

In these expressions, F_S is the spontaneous fission (SF) rate taking place in the item in the detector; ε is the neutron detection efficiency in counts per neutron for neutrons emerging from the reflector; M_L is the leakage neutron multiplication factor for the item-reflector combination; and ν_{Si} is the i[th] factorial moment of the normalized SF prompt neutron multiplicity emission distribution, $P_S(\nu)$. That is to say, $\nu_1 = \sum_{\nu=1}^{max} \nu.P_S(\nu)$, $\nu_2 = \sum_{\nu=2}^{max} \nu.(\nu-1).P_S(\nu)$, and $\nu_3 = \sum_{\nu=3}^{max} \nu.(\nu-1).(\nu-2).P_S(\nu)$, where max is the highest value of ν observed (note the quantities $\nu_n/n!$ are referred to as reduced factorial moments); $\alpha = F_\alpha.1/F_S.\nu_{S1}$ is the ratio of the random (in time) neutron to (SF,n) production inside the item where in the present context the random production includes (α,n)-reactions and delayed-neutrons following fission since the delayed neutrons do not contribute to short term (that is of the order of the system die-away time) fluctuations associated with the fission event; and f_d is the signal (or event) triggered gate utilization factor for doubles counting according to shift register logic.

It is interesting to expand the point model equations (which results in a form similar to that obtained from derivation before rearrangement to a compact stylized form). The subscript on M_L is dropped for convenience:

$$S = (\varepsilon.M).(F_S.\nu_{S1} + F_\alpha) \quad (3)$$

$$D = (\varepsilon.M)^2.f.\left[F_S.\frac{\nu_{S2}}{2} + (F_S.\nu_{S1} + F_\alpha).\frac{(M-1)}{(\nu_{I1}-1)}.\frac{\nu_{I2}}{2}\right] \quad (4)$$

Note, for convenience, the subscripts on f and M have been removed because they can be understood to be present by the context of the discussion. The factor (M - 1)/(ν_{I1} - 1) is being used as a proxy for the number of induced fissions per source neutron taking place inside the item.

Although it is rarely explained this way, the following can now be identified as important underlying determinants of behavior in the point model approximation where the reaction kinetics in the item are assumed to be instantaneous in comparison to the die-away time in the detector:

$$r_{e1} = M.(F_S.\nu_{S1} + F_\alpha) \quad (5)$$

$$\frac{r_{e2}}{2} = M^2.\left[F_S.\frac{\nu_{S2}}{2} + (F_S.\nu_{S1} + F_\alpha).\frac{(M-1)}{(\nu_{I1}-1)}.\frac{\nu_{I2}}{2}\right], \quad (6)$$

where these equations represent the first and second reduced factorial moment rates emerging from the item-reflector onto the detector. Because of the multiplication dependence, these are configuration specific, as noted earlier. The singles rate is linear in multiplication. Two environmental configurations (with and without Cd) will now be considered. The source term remains unchanged, and by design the fast-neutron detection efficiency can also be taken to remain the same.

For the singles rates with and without Cd, the following equations are derived respectively:

$$S_1 = M_1.\varepsilon.(F_S.\nu_{S1} + F_\alpha) \quad (7)$$

$$S_2 = M_2.\varepsilon.(F_S.\nu_{S1} + F_\alpha) \quad (8)$$

Various combinations can then be formed, for instance,

$$\frac{S_2-S_1}{S_1} = \frac{M_2-M_1}{M_1} \ , \quad (9)$$

which, for evaluation, reduces to

$$\theta = \frac{M_2}{M_1} = \frac{S_2}{S_1} \ . \quad (10)$$

The dilemma that is present in Bolind's work, and is left unanswered, is whether the observable metric θ is experimentally viable, robust, and informative. In particular, how does θ correlate to, say, fissile mass.

In the case of double counting, we have additional complications. For the Doubles rates with and without Cd, the following equations are derived respectively:

$$D_1 = \varepsilon^2.f_1.M_1^2.\left[F_S.\frac{\nu_{S2}}{2} + (F_S.\nu_{S1} + F_\alpha).\frac{(M_1-1)}{\left(\nu_{I1}^{(1)}-1\right)}.\frac{\nu_{I2}^{(1)}}{2}\right] \quad (11)$$

$$D_2 = \varepsilon^2.f_2.M_2^2.\left[F_S.\frac{\nu_{S2}}{2} + (F_S.\nu_{S1} + F_\alpha).\frac{(M_2-1)}{\left(\nu_{I1}^{(2)}-1\right)}.\frac{\nu_{I2}^{(2)}}{2}\right] \quad (12)$$

Firstly, even in the point model framework, the expressions (listed above) are cubic in multiplication, and so the relationship between the doubles rates in the two configurations is not separable in a simple way even if, say, M_2 and M_1 are proportionate to each other (i.e., $M_2 = M_1$). Secondly, although the point model is inadequate to represent it properly, it can be seen that even with fixed pre-delay and coincidence-gate settings, the gate utilization factors (i.e., coincidence gate fractions) will be different. This introduces another variable, which must be determined by calibration. And in practice because the returning neutrons will on the average induce fissions later in time compared to the primary source neutrons, the difference between D_2 and D_1 can be emphasized by using different pre-delay and gate width values. Thirdly, it must be acknowledged that the factorial moments of the induced fission neutron multiplicity distribution are not constant but instead depend on the spectrum of interrogating neutrons, which is softer without the Cd insert. The effective values to be used in any inversion process must be determined by detailed calculations or experimentally. Finally, it must be reiterated that the point model is inadequate to account for the temporal and spatial differences between the two measurement configurations. However, by referring to it, the project work has been able to introduce these key issues from a familiar vantage point.

Some sweeping broad generalizations are now going to be made on the basis that, for the experimental scenario of interest, all the items are of similar geometry (roughly constant coupling) and are deeply sub-critical (i.e., the probability of extended chains present in the returning neutrons is low).

Firstly, when extrapolated over all time (zero pre-delay and infinite gate width), the only difference between D_2 and D_1 is a consequence of the thermal neutrons returning from the reflector and inducing fission. It shall be assumed that M_2 and M_1 are proportionate for the sake of establishing the functional dependence. To first order, the strength of the thermal flux, ϕ, can be taken to be proportional to the primary source term boosted by multiplication. The induced fission strength is the product of the thermal flux and a coupling parameter, C. The product $C.\phi$ then takes the place of F_α in the doubles expression with a random driver. Thus, the following can be written:

$$D_2 - D_1 \approx (\varepsilon.M)^2.\left[0 + C'.M.(F_S.\nu_{S1} + F_\alpha).\frac{(M-1)}{(\nu_{I1}-1)}.\frac{\nu_{I2}}{2}\right], \quad (13)$$

where the " $\approx$ " symbol is used to denote approximate functional dependence and introduced the new coupling parameter C'.

By rearrangement,

$$\frac{D_2 - a.D_1}{S_1} \approx b.M^2.\frac{(M-1)}{(\nu_{I1}-1)}.\frac{\nu_{I2}}{2}\ , \quad (14)$$

where the scale factor a is introduced to account for the use of finite rather than infinite gating; b is the constant of proportionality (which neglects self-shielding in large dense lumps of fissile material); M is a measure of self-multiplication and the relation to fissile mass must be established; and the induced fission factorial moments are those appropriate to slow neutrons. This expression is a cubic in M and can be solved for M. If $(M-1)$ is close to zero, the expression is almost proportional to $(M-1)$. The experimental investigation of this type of semi-empirical forms such as this one is one motivation of the present study.

Four measured quantities have been combined to three to get a new metric for multiplication, but if the objective is to use this form by back substitution, then the issue still exists of having to determine F_α along with F_S. That is, a known α solution likely will be invoked in the case of Pu. In the case of SNF, α is very small (<1%) but M is very important ($M \sim 2\ to\ 4$), so ^{244}Cm mass (i.e., F_S) needs to be extracted. Therefore, a functional form along these lines may work well for the spent nuclear fuel NDA application.

1.5 ANALYSIS OF EXISTING DATA

Neutron counting rate data has previously been acquired under the NGSI Spent Fuel Program using a self-interrogation (active source term) passive neutron albedo reactivity (PNAR) method in a small item inventory counter (JCC-12) in response to North Ana pressurized water reactor (PWR) spent fuel pins (24 measurements) measured in the hot cells within Building 3525 at ORNL. The Cd ratio and Cd subtraction signatures were calculated for this existing data. The self-multiplication of pins is small, and therefore, the signal from the induced fission rate to the background spontaneous fission rate achievable is low. It was concluded that, although a net, useable signal was present, there was not enough variation in the signature as a function of fissile mass to draw any substantive conclusions. Furthermore, the measurements were performed on pin sections of varying lengths, which complicates quantitative analysis. Therefore, a measurement campaign was required to collect new data with a measurable signal as a function of varying fissile mass.

2. PROJECT EXPERIMENTAL MEASUREMENT CAMPAIGN

The project experimental measurement campaign was performed in the NDA Systems Laboratory at ORNL. An initial design stage was performed using simulation. Measurements were then performed in three stages: (1) establishing counter settings; (2) sampling the time profile distribution; and (3) collecting signature data as a function of fissile ^{235}U mass. The experiment design, measured data, analysis results, and findings from the measurement campaign are presented here.

2.1 NDA SYSTEM AND EXPERIMENTAL CONFIGURATION

2.1.1 Large Volume Active Well Coincidence Counter (LAWCC)

The Large Volume Active Well Coincidence Counter (LAWCC), shown in Fig. 3, was the NDA system chosen and configured for the measurement campaign. The LAWCC is the highest efficiency neutron well counter currently available at ORNL with a total neutron detection efficiency ~29% to a ^{252}Cf neutron energy spectrum, and die-away time of 70.6 μs [2]. This neutron detection efficiency is achieved by a total of 48 ^{3}He gas-filled proportional tubes in the counter body (24 ^{3}He tubes in the inner detector ring and 24 ^{3}He tubes in the outer detector ring), each with a 1in. diameter and 4 atm fill-gas pressure. Measurements were performed with the counter itself configured and operated in the passive mode, i.e., with the AmLi (α,n) interrogation sources removed and by replacement of the high-density polyethylene (HDPE) end-plugs with graphite end-plugs. However, to achieve the conditions necessary for albedo active neutron interrogation, measurements were performed using a ^{252}Cf source of strength ~1.5×10^{5} ns^{-1} positioned in the center of the assay cavity, directly underneath each item being measured in close geometry. A counter insert was also required to generate the re-entrant neutron flux, which is described in Sect. 5.2.

Fig. 3. The LAWCC stationed in the ORNL NDA Systems Laboratory.

2.1.2 Data Acquisition Electronics

Counts from neutron detection events were recorded using a JSR-15 multiplicity shift register (MSR), shown in Fig. 4. Data acquisition using the JSR-15 was controlled using the IAEA Neutron Coincidence Counting (INCC) software (version 5.1.2) [15]. All measurements were performed in the multiplicity counting mode (rather than the coincidence counting mode) to determine the singles, doubles, and triples neutron counting rates from the measured multiplicity histograms. The Triples were not used for this study but were measurable and are available in the data files for future safeguards technology development work.

Fig. 4. JSR-15 multiplicity shift register.

2.2 EXPERIMENT DESIGN USING SIMULATION

2.2.1 LAWCC Insert

An insert was designed for the LAWCC using simulation and built for the experimental measurement campaign to achieve the conditions necessary for albedo active neutron interrogation. This design is based on the concept of the Passive Neutron Multiplicity Counter (PSMC) insert designed by Menlove and Beddingfield [1] for one of the first PNAR experiments applied to safeguards neutron counting. However, our experiment differs in focus and application from the original experiment. In this work, a lower detection efficiency counter was used and measurements were made of fissile ^{235}U standard cans using ^{252}Cf as an active interrogation source, whereas in the original work, measurements were made of fuel rod elements using ^{252}Cf to simulate self-interrogation by the intrinsic spontaneous fission neutrons emitted from ^{244}Cm. In this work, the data were analyzed using both the original Cd ratio signature and the proposed Cd subtraction signature for comparison. A number of pre-delay settings were also considered. Previous work considers the Cd ratio only at a single gate and pre-delay setting.

There are three basic components of the LAWCC insert:

(1) a moderator,
(2) a reflector [may be the same as (1)], and
(3) a slow neutron absorber (removable item Cd liner).

The LAWCC insert enables measurements to be performed under two conditions: with and without a thermal neutron albedo. The first measurement is performed without component (3), the item Cd liner, in place [this is labeled "item Cd liner" to keep it distinct from the fixed Cd liner that lines the assay cavity in the main body of the counter]. To generate the re-entrant neutron flux (albedo), it is necessary to surround the assay item itself with moderator/reflector components (1) and (2). The ^{252}Cf active interrogation source is placed directly underneath the item, and ^{252}Cf spontaneous fission neutrons may enter the item and induce fission. Following the primary induced fission in the item, prompt fission neutrons emitted from the item are either detected (fast neutrons), moderated, and returned to the item by reflection to induce further fission or undergo parasitic capture in the HDPE. Due to the thermal albedo neutron-induced fission, this measurement condition represents the largest item multiplication and the greater signal of the two measurements (highest correlated neutron counting rates).

For the second measurement condition, a slow neutron absorber (item Cd liner), is placed between the item and the moderator/reflector to absorb the thermal and epi-thermal component of the returning neutron flux. This environmental change and resulting reduction in the slow component of the re-entrant neutron flux (due to absorption of the returning albedo neutrons) lower the item multiplication compared to the first measurement condition. Any measured signature should be able to reveal the difference in item multiplication under these two conditions. The absolute difference in the signal itself ought to represent the difference in the item multiplication under these two conditions and thus provide a measure of fissile mass.

The LAWCC insert was designed using the radiation transport code MCNPx. Simulation calculations were performed to optimize the moderator and reflector geometry, as well as the thickness of the item Cd liner. An existing MCNPx model developed by McElroy [2] was adapted to include this insert in the center of the assay cavity surrounding the assay item. The LAWCC model is shown in Fig. 5. Simulations were run for the counter configured in the passive mode to replicate the experimental geometry. The item holder included a small ^{252}Cf interrogation source holder for good reproducibility of the item and interrogation source positioning. (Note that, where possible, the experiment configuration used for this project maintained the configuration used for the DMM project, in case the data measured here are also useful for that method and vice versa.)

The insert geometry was composed of nested rings, or sleeves, of HDPE. The inner ring had an inner diameter of 10 in., and each ring was 0.5 in. thick. This thickness of HDPE was chosen to facilitate the straightforward machining of the final product. The item Cd liner is external to the ^{252}Cf source and positioned on the item side of the reflector (inside the polyethylene rings). Both 1 mm and 2 mm Cd liners were simulated. Source neutrons should not be thermal (moderated) when they leave the source to provide fast-neutron interrogation and, therefore, a higher probability of penetrability into the center of the item. The item Cd liner, therefore, surrounds the item, but not the ^{252}Cf source.

Regarding material design choices, the moderator and reflector components can be the same material and thus a single component if either HDPE or graphite is chosen. It would be equally valid to use two different materials to provide moderation and reflection, for example, HDPE and steel, respectively. However, HDPE was chosen to keep the design simple, and also due to it being lighter in weight and a more effective moderator (higher neutron energy loss per unit scatter).

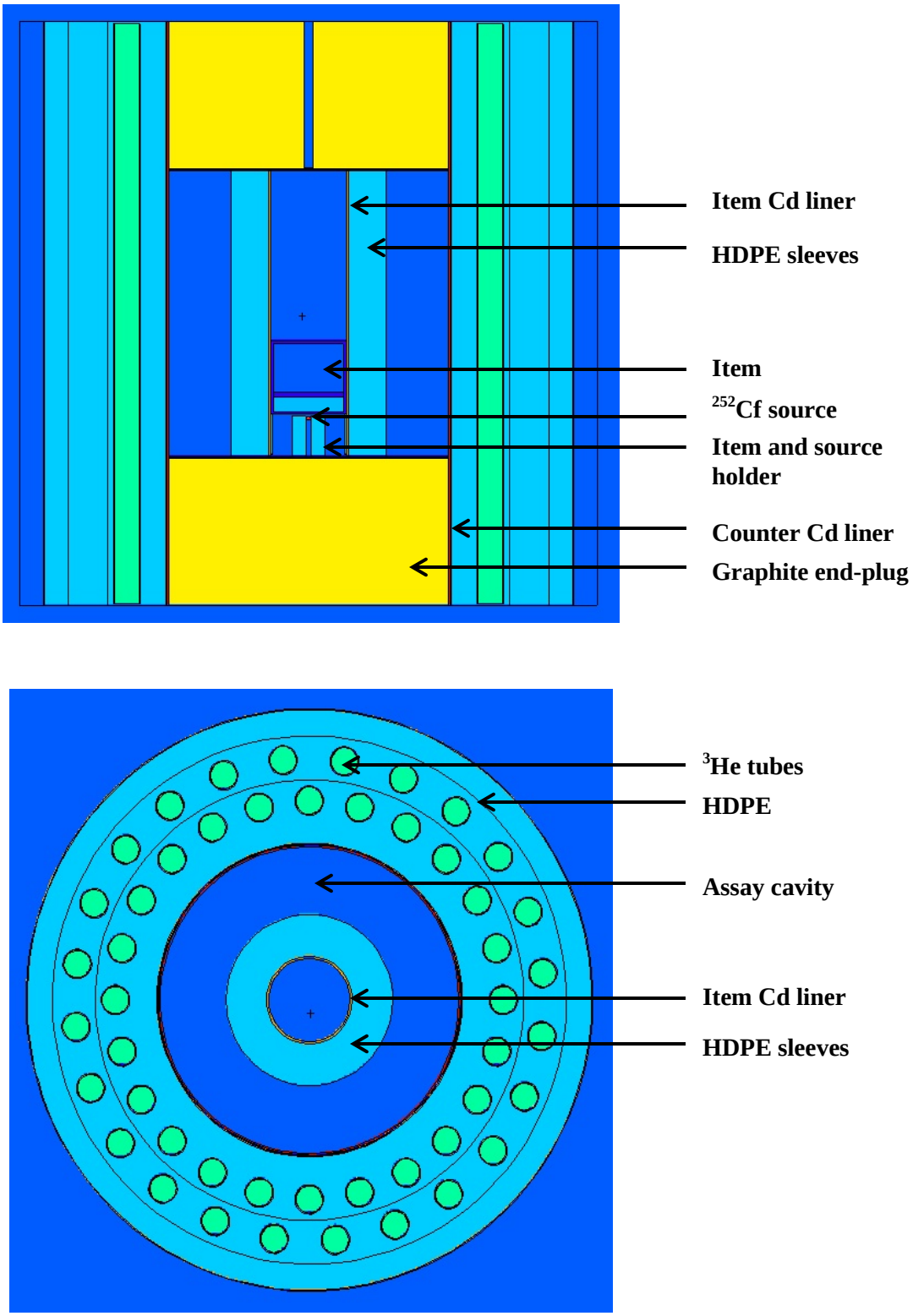

Fig. 5. MCNPx model geometry of the LAWCC with insert. Cross section of the LAWCC with insert viewed from the side (top). Cross section of the LAWCC with insert viewed from the top looking down into the assay cavity (bottom).

2.2.2 Design Calculations Using MCNPx

The main goal of the optimization calculations was to ensure that a measurable albedo neutron effect could be observed for the purpose of predicting empirical performance. For the optimization of the LAWCC insert design, the reflecting surface (HDPE) should return a substantial fraction of the emitted neutrons to the item and lead to re-interrogation of the item from the thermal neutron albedo. The aim is to return a large fraction of the thermal neutrons (i.e., moderate and reflect in the polyethylene but not absorb) because the fission cross section in the fissile ^{235}U material peaks at thermal neutron energies. Figure 6 shows the Cd ratio and Cd subtraction signatures as a function of HDPE thickness. The HDPE thickness was varied in increments of 0.5 in. up to 2 in. A control measurement was also simulated with no HDPE in place. Simulations were repeated at Cd liner thicknesses of 1 mm and 2 mm.

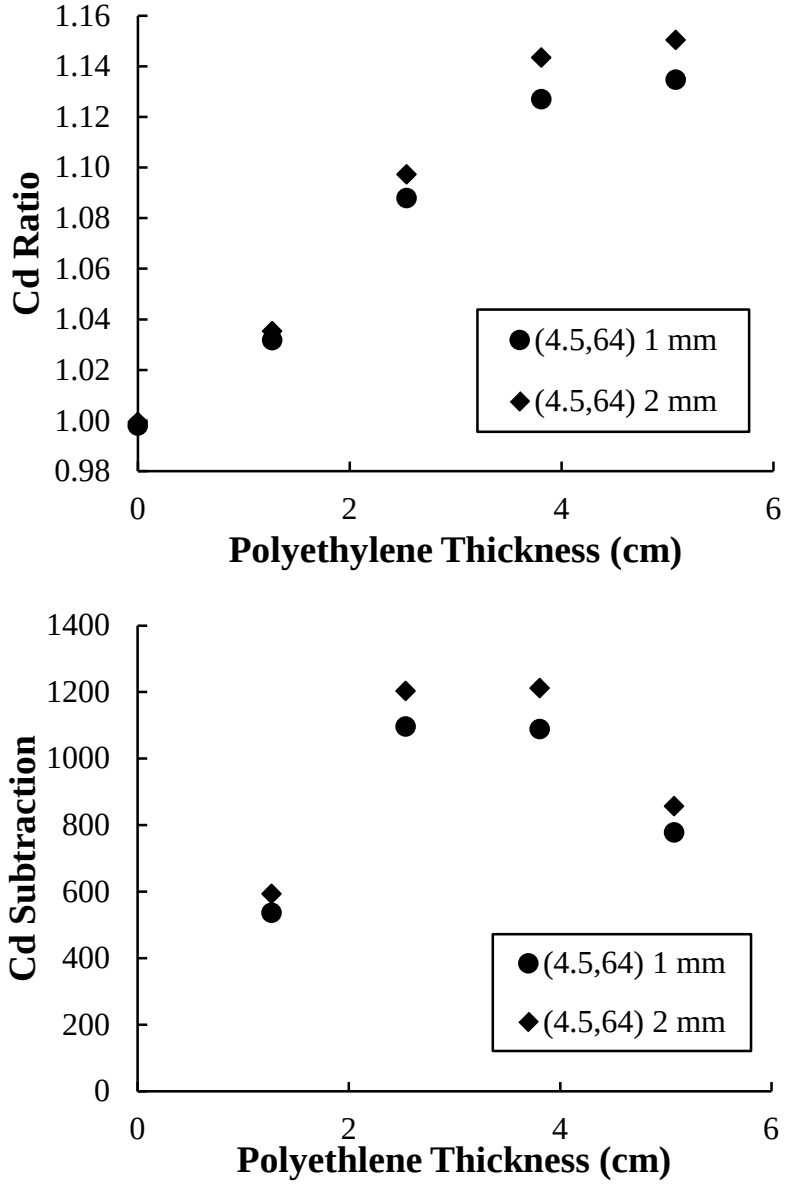

Fig. 6. Cd ratio and Cd subtraction signatures as a function of polyethylene thickness. Cadmium ratio as a function of polyethylene thickness (top) and Cd subtraction as a function of polyethylene thickness (bottom).

It can be observed in Fig. 6 that the simulated doubles Cd ratio showed up to a 15% effect. The Cd ratio was greatest at a HDPE thickness of 2 in. The doubles Cd subtraction also showed a measurable effect of up to 1200 counts. The Cd subtraction reached a maximum value at a HDPE thickness of 1.5 in. and then decreased at 2 in. The use of a 2 mm item Cd liner compared to a 1 mm Cd liner increased the signal for both signatures. Therefore, it was concluded that the signal difference would be measurable empirically. A HDPE thickness of 1.5 in. and item Cd liner thickness of 2 mm were chosen for the final insert design to optimize both signatures.

The prompt, fast component of the ^{252}Cf source neutron flux and the induced fission neutrons will reach the detectors during each measurement. Ideally, this fast component of the response should be the same with and without the item Cd liner in place. In reality, the detection efficiency is modified by the item Cd liner and environmental conditions. Figure 7 shows the calculated neutron detection efficiency as a function of polyethylene thickness. The change in the neutron detection efficiency as a function of polyethylene thickness is cause by the changing neutron energy spectrum incident on the detector and overlap with the detector cross-section, which changes the fraction of neutrons in the sensitive energy region. Figure 7 also provides a demonstration of the total efficiency changes with and without Cd. The neutron detection efficiency changes in the Cd and no Cd case because of the spatial-energy coupling between zones (i.e., item, reflector, cavity, and detector). However, overall, there was greater variation in the neutron detection efficiency with polyethylene thickness than there was between the two measurement conditions with and without Cd.

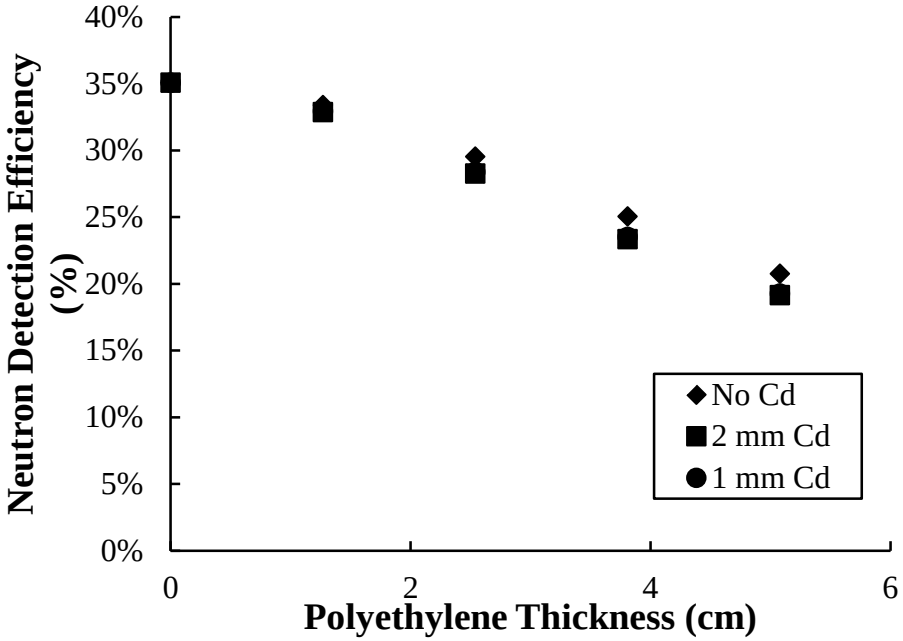

Fig. 7. Neutron detection efficiency as a function of polyethylene thickness.

The final comparison, which is perhaps the most instructive, was to compare thermal and fast fission neutron gains in the system. Although the thermal and fast component of the albedo neutron flux were not tallied directly in simulation using energy binning (which is considered to be a useful future extension to this work), the fission neutron gains in the ^{235}U material in the item and the ^{238}U material in the item could be tallied separately. This reveals the same physics that the predominant effect is the removal of thermal neutrons because an increase in induced fission in ^{235}U will be proportional to the number of thermal neutrons inducing fission, and an increase in induced fission in ^{238}U will be proportional to the number of fast neutrons inducing fission. This comparison enables the tracking of changes in the thermal neutron component of the re-interrogation flux.

The signature that tracks this effect is the more correct signature for thermal albedo-neutron multiplication. Figure 8 shows the fission neutron gain as a function of polyethylene thickness and with and without Cd for both the ^{235}U and ^{238}U in the item. This graph provides an indirect indication of how the thermal and fast component of fission trend with polyethylene thickness (thermal component increased to increase signal from fissile material).

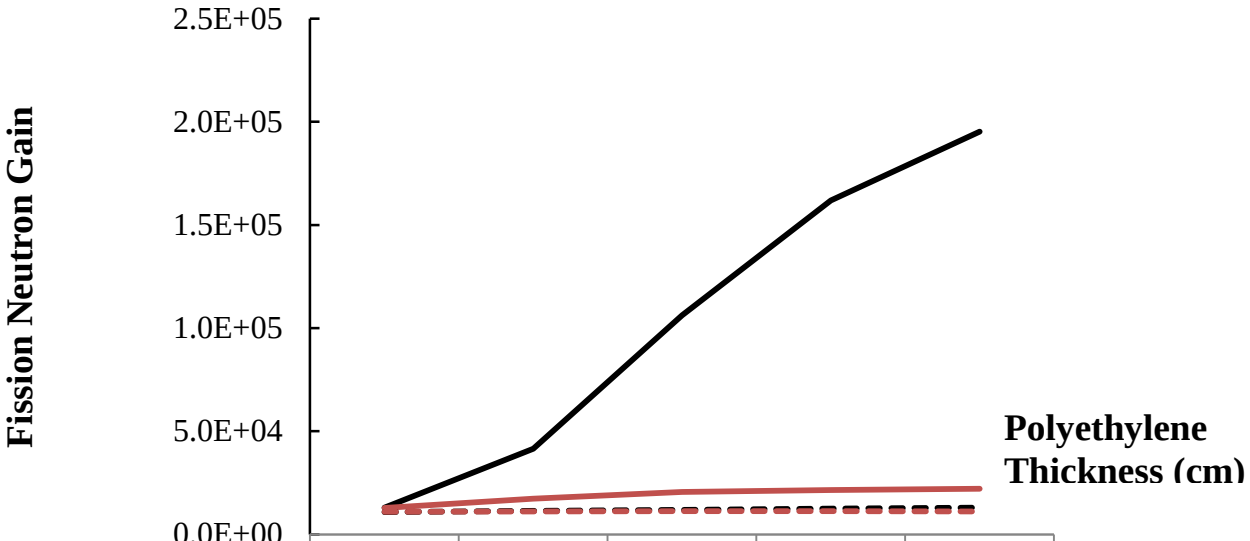

	0.00	1.27	2.54	3.81	5.08
U-235 - No Cd	1.30E+04	4.15E+04	1.06E+05	1.62E+05	1.95E+05
U-235 - 2 mm Cd	1.29E+04	1.72E+04	2.06E+04	2.15E+04	2.21E+04
U-238 - No Cd	1.08E+04	1.14E+04	1.19E+04	1.26E+04	1.30E+04
U-238 - 2 mm Cd	1.10E+04	1.11E+04	1.13E+04	1.12E+04	1.11E+04

Fig. 8. Fission neutron gain as a function of polyethylene thickness and Cd liner.

The presence of a removable Cd liner should, therefore, prevent this re-interrogation by absorbing the thermal component of the thermal neutron albedo. In the ^{235}U case with no item Cd liner present, the thermal neutron albedo is demonstrated by the thermal fission neutron gain. Note that the slope decreases slightly between 1.5 in. and 2 in. of HDPE. Therefore, there is less gain for the extra 0.5 in. of HDPE.

The Cd liner should absorb the returning fast component of the albedo, and this is demonstrated to be the case by the similarity in the ^{238}U Cd and no Cd cases. There is a small but finite probability of fast fission in ^{235}U, and therefore the induced fission does not reduce to zero with the presence of the Cd liner, but a small fission neutron gain can be observed. In future, it would be reasonable to tally the energy-dependent induced fission to check that fast fission cancels out in the ratio since the signature should be a measure of fissile content.

2.2.3 LAWCC Insert Final Design

As described, the insert was designed to fit around the ORNL set of enriched uranium standard cans (see Sect. 2.5). Each measurement was performed with the polyethylene component of the insert in place and repeated with and without the item Cd liner. Figure 9 shows the individual components of the LAWCC insert, which was deliberately designed and built to be fully reconfigurable should other HDPE thicknesses be required for future experiments of this type, or for benchmarking activities. Figure 10 shows the complete LAWCC insert (a) without the Cd in place (Cd removed) and (b) with the Cd liner in place.

Fig. 9. Components of the LAWCC insert (configurable). Three polyethylene sleeves are shown (left) with one 2 mm Cd sleeve (right) that comprises the LAWCC insert. The Cd sleeve is machined to fit inside the concentric, nested polyethylene sleeves, each of 0.5 in. thickness. The uranium standard can used for the initial measurements is positioned in front of the insert components for scale.

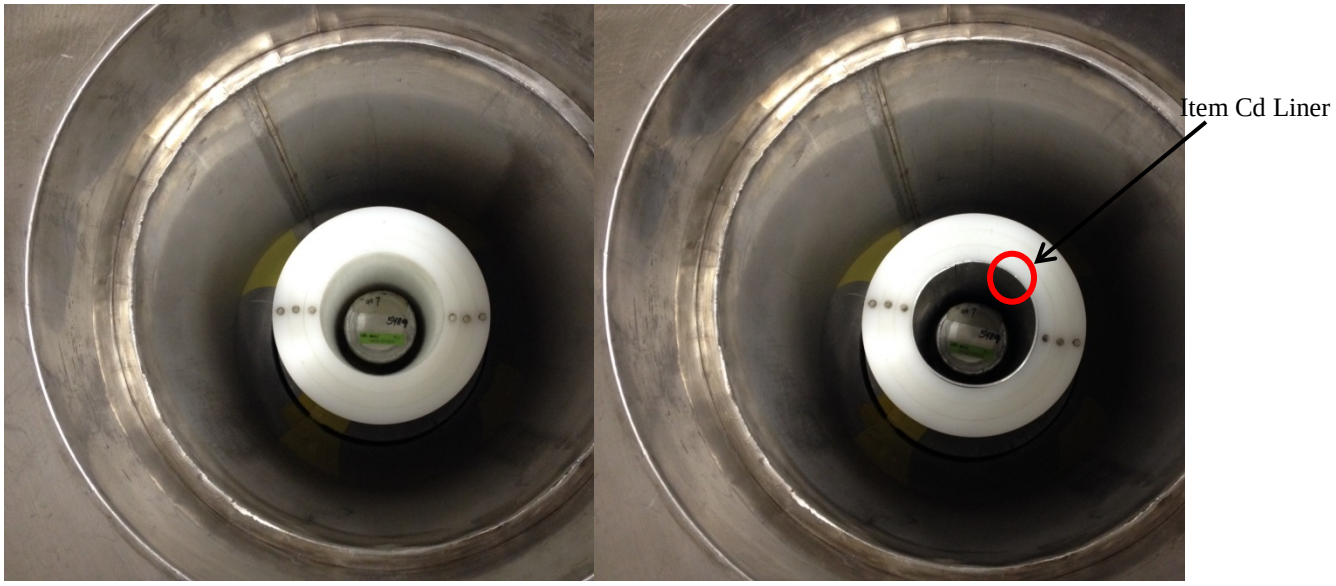

Fig. 10. Item without (left) and with Cd insert (right). The photographs are taken looking down into the LAWCC cavity. The insert is in place with Cd removed (left) and with Cd in place (right). The insert sits around the item being measured. The detector Cd liner is not visible behind the protective liner.

2.3 HIGH-VOLTAGE BIAS SETTING

The optimal high-voltage (HV) setting of the bias supply is one of the basic operational parameters for neutron correlation counters, including the LAWCC. The appropriate setting for the HV bias supply was determined by the assay of a ^{252}Cf source and incrementing the voltage. The ^{252}Cf source was placed in the source holder, centered at the bottom of the counter assay cavity (well). The 1.5 in. polyethylene sleeve was also present in the counter cavity since this comprised the final measurement configuration. The voltage was incremented by 5 V between 1560 V and 1860 V. The INCC software features a utility to automate this incremental change in voltage. Figure 11 shows the singles rate (counts · s^{-1}) recorded as a function of bias setting or voltage (V).

The traditional HV bias setting is ~40 V above the "knee" for ^{3}He gas-filled proportional counters. This places the operating point on the flattest part of the plateau. In turn, this reduces the sensitivity of the detection efficiency to variations in HV setting and to gamma rays (the influence of which tends to shorten the HV plateau). The knee can be observed at 1680 V. The bias setting was, therefore, selected as 1720 V. It can be observed in Fig. 10 that 1720 V places the bias setting in the most stable region of operation.

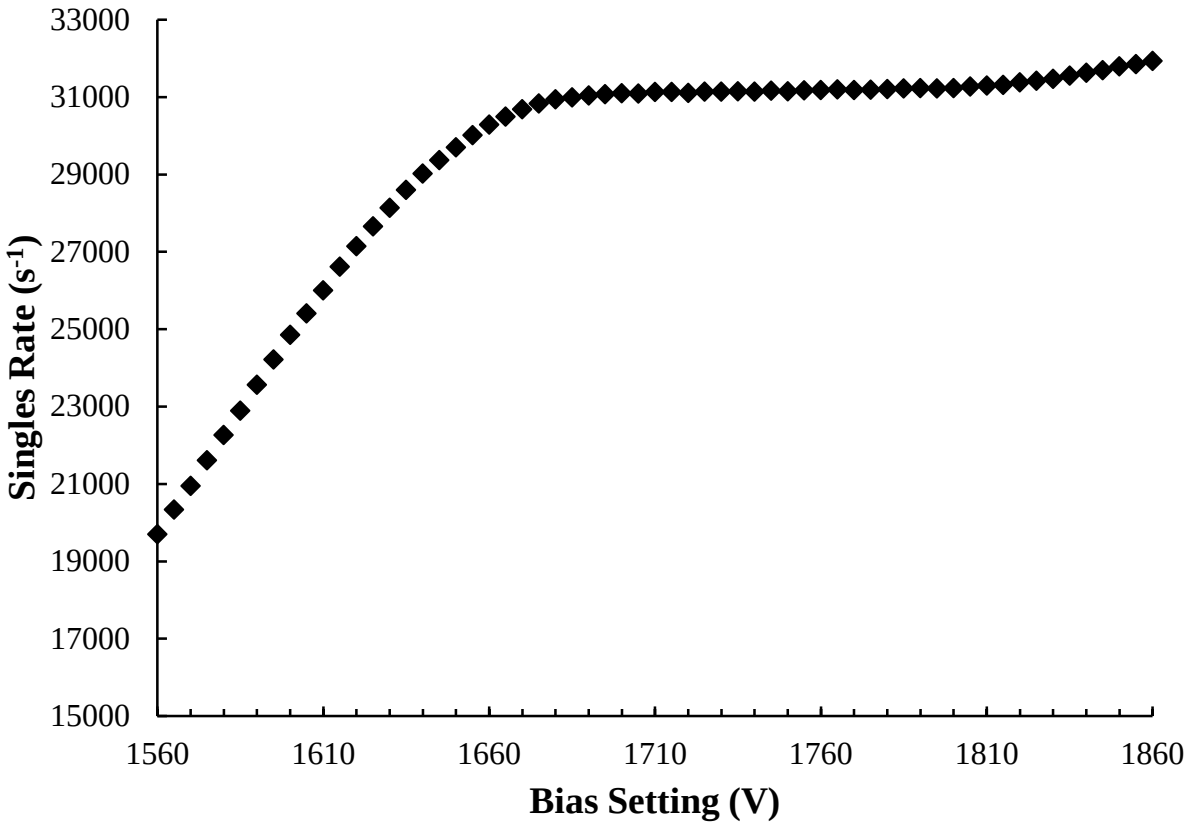

Fig. 11. HV Bias Setting. Singles rate (s^{-1}) as a function of bias setting or voltage (V).

From a field-implementation standpoint, it is important to note that the HV bias setting is dependent on the type of item being measured. For example, in the case of the measurement of spent nuclear fuel using the PNAR technique, the bias setting may need to be reduced (operation below the knee) due to the large flux from fission-product gamma rays.

2.4 BACKGROUND MEASUREMENT

It was necessary to quantify the background count rate with good precision, so as not to impact the precision of the measured neutron counting rates following background subtraction. For safeguards assay, the background counts are generally small compared to the item counts. Therefore, a shorter background count is sufficient (in comparison to that required for waste assay, for example, when counting near to the minimum detectable activity, or MDA). At the beginning of the measurement campaign, a passive background measurement was performed for 12 h using 1440 cycles of 30 s cycle time. Short cycles (30 s) are chosen to reveal any rare or unexpected fluctuations or spikes in the background counting rates, such as those caused by cosmic-ray bursts or electronic noise (such as noise due to radio-frequency generators or motors in nuclear facilities). Short cycle times thus enable the software to reject large cosmic-ray events based on a statistical filter [16] to prevent them from contributing to the measured count rate. The background singles and doubles rates, with uncertainties, are recorded in Table 1.

Table 1. Background neutron counting rates and uncertainties

Singles			Doubles		
Rate (s^{-1})	**Uncertainty (s^{-1})**	**Relative Uncertainty (%)**	**Rate (s^{-1})**	**Uncertainty (s^{-1})**	**Relative Uncertainty (%)**
6.154	0.014	0.227	0.111	0.002	1.802

Note: Rates and uncertainties quoted with the same level as precision as given in the INCC file.

2.5 CALIBRATION STANDARDS

Table 2 provides details of the set of uranium (U_3O_8 powder) standard reference material (SRM 969) available in the Safeguards Laboratory at ORNL. These standards were fabricated by the former National Bureau of Standards (NBS) [now the National Institute of Standards and Technology (NIST)] New Brunswick Laboratory (NBL) and were employed for this campaign of measurements. Uranium-235 enrichment and mass (^{235}U and total mass) are given. A blank (zero mass) standard also exists for comparison. During the final experiment, Cd ratio and Cd subtraction signatures were acquired for all available calibration standards. Larger mass items would be desirable but were not readily available.

Table 2. Uranium standards from NBS and NBL measured in the LAWCC

Standard Description	^{235}U Enrichment (%)	Total Mass ^{235}U (g)	Total Mass U (g)
NBS 031-078 (Depleted)	0.31	0.52	169
NBS 295-078 (Enriched)	2.95	4.99	169
NBS 446-078 (Enriched)	4.46	7.54	169
NBL-0001	20.11	39.10	194.43
NBL-0002	52.49	101.72	193.79
NBL-0003	93.17	181.15	194.43

2.6 COUNT TIME DETERMINATION: EVALUATION OF COUNTING STATISTICS

For this type of albedo NDA measurement, counting times must be sufficient to enable good precision (<2% relative uncertainty) in the Cd ratio and Cd subtraction quantities, in addition to enabling good precision on the individual neutron counting rates. This is unlike the situation for standard gross neutron or neutron coincidence counting, where the precision in the individual neutron counting rates is the uncertainty value of primary interest. Therefore, an evaluation of experimental counting statistics was performed at the beginning of the measurement campaign, prior to performing any assay measurements, to understand the precision achievable in 900 s, 1800 s, and 3600 s count times. Count times greater than 3600 s lead to an unnecessarily long measurement campaign and deem the method unsuitable for practical field applications.

The highest enriched (94 wt % ^{235}U) uranium standard was chosen for these measurements with the ^{252}Cf active interrogation source in place. Measurements were performed of the singles and doubles neutron counting rates as a function of counting time, using the standard IAEA gate settings of a 4.5μs pre-delay and 64 μ s gate width (triples is not being considered in this approach). Count times used were 900 s (typical assay time), 1800 s, and 3600 s. The relative uncertainties in the singles rates (with and without Cd), doubles rates (with and without Cd), doubles Cd ratio, and doubles Cd subtraction were determined as a function of count time. The Cd ratio and Cd subtraction were derived from the measured doubles neutron counting rates using Eqs. (15) and (16), respectively. Note that Eq. (16) is equivalent to Eq. (13) and is a simplified version of Eq. (14), documented in Sect. 1.4.

$$CR = \frac{D}{D'} \tag{15}$$

$$CS = D - D', \tag{16}$$

where D is the doubles rate without Cd present and D' is the modified (or perturbed) doubles rate with Cd present.

Uncertainties in the Cd ratio and Cd subtraction were propagated using Eqs. (17) and (18).

$$\sigma CR = \sqrt{\left(\frac{\sigma D}{D}\right)^2 + \left(\frac{\sigma D'}{D'}\right)^2} \cdot CR \tag{17}$$

$$\sigma CS = \sqrt{\sigma D^2 + \sigma D'^2} \tag{18}$$

The results are presented in Tables 3 and 4.

Table 3. Raw neutron counting rate data with uncertainties as a function of count time, with and without Cd

Configuration	t (s)	Singles (s^{-1})	Uncertainty (s^{-1})	Relative Uncertainty (%)	Doubles (s^{-1})	Uncertainty (s^{-1})	Relative Uncertainty (%)
No Cd	900	33578.4	8.0	0.024	8572.5	17.1	0.20
Cd	900	31901.5	9.0	0.028	7802.2	15.5	0.20
No Cd	1800	33546.4	5.8	0.017	8553.3	15.0	0.18
Cd	1800	31905.2	4.9	0.015	7787.8	12.8	0.17
No Cd	3600	33545.4	4.3	0.013	8554.3	9.7	0.11
Cd	3600	31910.7	3.9	0.012	7824.0	7.6	0.10

It can be concluded from the data in Table 3 that the relative uncertainties in the singles and doubles neutron counting rates were <1% for all measurement configurations and counting times.

Table 4. Cd ratio and Cd subtraction derived signatures with uncertainties as a function of count time

t (s)	Cd Ratio	Uncertainty	Relative Uncertainty (%)	Cd Subtraction	Uncertainty	Relative Uncertainty (%)
900	1.099	0.003	0.282	770.361	23.104	2.999
1800	1.098	0.003	0.241	765.511	19.766	2.582
3600	1.093	0.002	0.150	730.256	12.352	1.691

Table 4 shows that the relative uncertainties in the Cd ratio were <0.3% for all counting times. The uncertainty in the Cd subtraction was 3% at 900 s and decreased to <2% at 3600 s. Therefore, it was concluded from these measurements that 900 s was a reasonable count time for exploring the trends in many of the settings (i.e., gate width and pre-delay), but a final data set would be taken using 3600 s count times.

2.7 OPTIMIZATION OF POLYETHYLENE THICKNESS—BENCHMARKING THE SIMULATION RESULTS

As described in Section 3.2, the optimal thickness of HDPE for the LAWCC insert was determined in simulation to be ~1.5 in. Measurements were performed of the high-mass 94 wt% ^{235}U uranium can using a count time of 900 s to optimize the thickness based on the Cd ratio and Cd subtraction signatures. The can was placed in the source holder in the bottom center of the assay cavity. Measurements were performed with and without the item Cd liner present. As predicted in simulation, the Cd subtraction signature reaches a maximum value (with lowest relative uncertainty) at a HDPE thickness of 1.5 in. It can be concluded from this data that there is a measurable signal with viable statistics, even in this low efficiency counter. An optimal HDPE thickness of 1.5 in. was also determined by experiment.

Table 5. Cd ratio and Cd subtraction signatures as a function of HDPE thickness

HDPE Thickness (in.)	Cd Ratio	Uncertainty	Relative Uncertainty (%)	Cd Subtraction	Uncertainty	Relative Uncertainty (%)
0.5	1.025	0.002	0.233	349.033	32.325	9.261
1.0	1.066	0.003	0.284	705.636	31.595	4.478
1.5	1.099	0.003	0.282	770.361	23.104	2.999
2.0	1.110	0.004	0.320	617.163	19.010	3.080

2.8 PRE-DELAY SETTING—TRADITIONAL METHOD

Historically, the pre-delay is set to minimize bias due to the recovery of the detector electronics (amplifier/discriminator board). The traditional method of pre-delay setting for a neutron coincidence counter is to fix the gate width at the historical IAEA setting of 64 μs and to increment the pre-delay by 0.5 μs between 0.5 μs and 5 μs to observe how the doubles trend with pre-delay. The original reason for this method is to ensure that the pre-delay is long enough to minimize bias due to the recovery of the detector electronics at short timescales following the trigger event. At the same time, the pre-delay must be short enough so that a large proportion of coincidences are not lost. In other words, the coincidences sampled by the coincidence gate width setting as a fraction of all available coincidences (coincidence gate fraction) should be maximized. Figure 12 shows the relative doubles rate (doubles rate relative to the doubles rate at the lowest pre-delay setting of 0.5 μs) as a function of pre-delay.

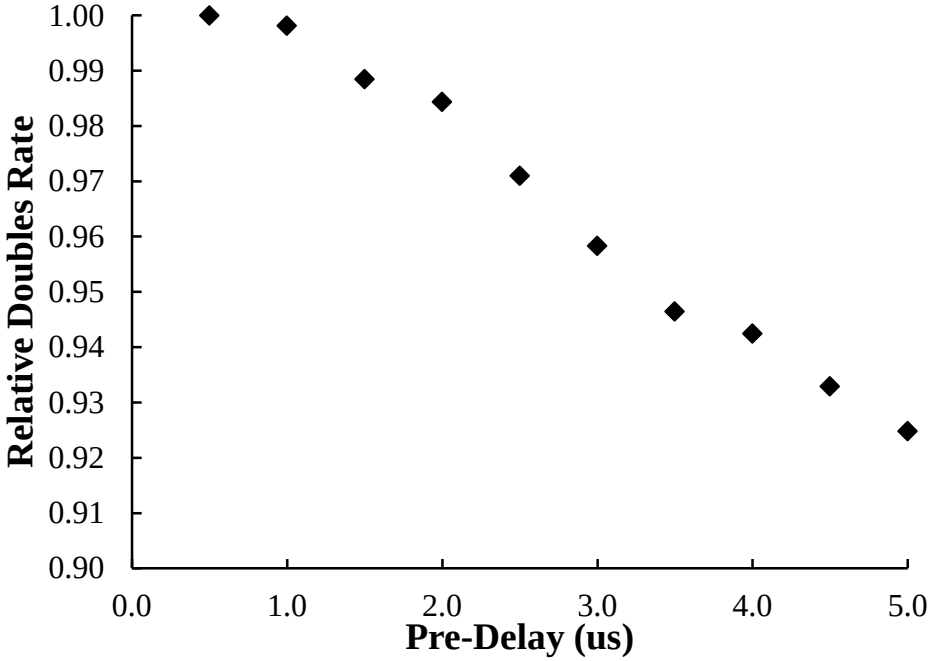

Fig. 12. Pre-delay setting (traditional method). Relative doubles rate as a function of pre-delay (μs).

This data was obtained from the assay of the ^{252}Cf interrogation source and the high-mass 94 wt% ^{235}U uranium can, using a count time of 900 s for each pre-delay setting (without Cd). The turnover at zero to low pre-delay is likely due to dead time and amplifier baseline restoration. Dead time is greatest for neutron detections following the initial spontaneous fission event due to a high instantaneous neutron counting rate caused by the detection of prompt fission events from the ^{252}Cf source.
This data demonstrates that the counter is functioning as expected but does not yield information on setting up the counter or determining the correct settings to optimize and calibrate for the Cd subtraction or Cd ratio. Further, this graph does not inform us of the "right" value of the pre-delay setting. For example, it is not obvious from this graph that the experimental setting should be the traditional IAEA setting of 4.5 μs. It is valid to set the pre-delay at 4.5 μs, but this is clearly a conservative setting. Therefore, this method currently remains a historical diagnostic check, rather than adding value to the determination of individual signatures. However, the original method was designed for coincidence counting and optimizing the doubles rate using ^{252}Cf only. It was not designed to account for temporal behavior within the coupled source-item-counter system. Purely for consistency with the IAEA traditional settings, a pre-delay setting of 4.5 μs was chosen for the final experiment to generate the signature data.

2.9 PRE-DELAY SETTING—NEW TIME PROFILE METHOD

This experiment represents the first experimental data set that has considered both the Cd ratio and Cd subtraction over a range of pre-delay settings. As demonstrated by the traditional pre-delay setting method described in Sect. 2.8, the time behavior of an NDA system, and thus our ability to extract the optimal signatures during calibration, can be hidden by routine calibration procedure. Prior work on albedo interrogation [10, 17] indicated that there could be a tangible benefit from delaying the coincidence gate width in time using an extended pre-delay. This benefit would be an improved ability to sample the detected neutron events of interest, i.e., detected neutron events emitted during induced fission in the item as a result of albedo neutron re-interrogation of the item. This is due to the fact that albedo neutron re-interrogation is a slightly delayed process compared to the primary fission from ^{252}Cf active interrogation because of the time required for the ^{252}Cf spontaneous fission neutron-induced fission neutrons to exit the item, moderate in the HDPE, and be reflected by the HDPE back in to the item.

The objective of this experiment was, therefore, to sample the time profile distribution of the detected neutron events. Generating such a distribution would improve understanding of the time behavior and reaction kinematics within the coupled system. Further, this type of approach would improve understanding of the optimal gating structure required to acquire the signal of interest. This was achieved by fixing the coincidence gate width to a small value (representative of the bin size of the histogram) and by sampling the time profile by moving the gate out in time. A gate width of 4 μs was chosen for this experiment, and the pre-delay was incremented by the value of the gate width for each measurement (data point). Repeating these measurements with and without Cd should yield the time profile of the signal buildup and decay for each physical process, represented by the Cd subtraction or difference.
Table 6 shows the pre-delay and gate width pairs used for each measurement.

Table 6. Pre-delay, gate width pairs

(Pre-Delay, Gate Width) (μs)
(2,4) μs
(6,4) μs
(10,4) μs
(14,4) μs
(18,4) μs
(22,4) μs
(26,4) μs
(30,4) μs
(34,4) μs
(38,4) μs
(42,4) μs
(46,4) μs
(50,4) μs

This method enabled the time distribution to be sampled with fine resolution. This method reveals the system time behavior, whereas the standard fixed pre-delay setting and long coincidence gate width method reveals nothing about the time behavior of the system over timescales shorter than the counter die-away time. Note that this would be one single measurement in list mode that could be reanalyzed using multiple pre-delay settings and gate widths.

The reason that this approach works is because the coincidence gate fraction (i.e., fraction of coincidences detected out of all available coincidences) will change as a function of time. Initially, more coincidences will be available for detection from the ^{252}Cf spontaneous fission source neutron-induced fission events. Slightly delayed in time, more coincidences will be available from the albedo neutron-induced fission as a result of the re-entrant neutron flux. In the measurement condition with the item Cd liner in place, the thermal albedo neutrons are absorbed and do not contribute to the signal. Figure 13 shows the doubles neutron counting rates with and without Cd as a function of pre-delay.

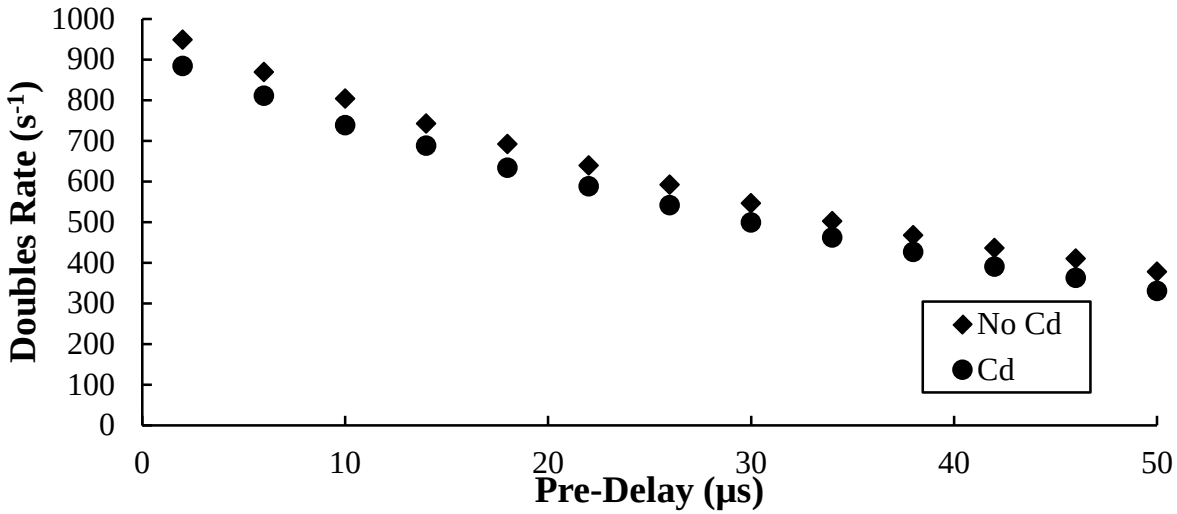

Fig. 13. Doubles rate as a function of pre-delay. This is the primary data.

Figure 13 shows the primary data that were measured. The doubles neutron counting rates represent the fundamental behavior and time profile of the neutron counting rates when sampled with a fixed 4 µs gate width moved out in time by varying the pre-delay. This fine gate was chosen to maximize the resolution in sampling the time profile distribution. Figure 13 essentially represents the histogram of coincidence events in time, with bin widths equal to the coincidence gate width of 4 µs.

Several observations can be made from Fig. 13. It is the difference between the two curves in Fig. 13, that is, the difference in the doubles with and without Cd, which reveals the amount of multiplication in the system. However, in the case of this item, it is a small difference and is somewhat "washed out" or drawn out by the time characteristics of the detector. Not only is the magnitude of the difference but also the shape difference in these two curves is key. However, the shape difference is small, which is likely due to smoothing out by the detector. A longer count time or higher efficiency detector is needed to observe the difference. There is not a strong difference in the shape of the two curves. However, this may change with more highly multiplying items. In this work, the sample size was small. The doubles curve without Cd is the sum of the detected source neutron events and the detected induced fission events. Since the induced fission events represent a smaller proportion of the overall signal, there is no obvious structure from the time behavior in the doubles curve itself, other than the fact that the difference between the two curves appears to change with time. For future work, it would be interesting to understand what happens on a longer timescale and investigate the effect of increasing the pre-delay further.

The Cd liner in the body of the LAWCC was left in place to maintain similar detection efficiency between these two measurement conditions. Although the neutron detection efficiency to neutrons in the region of the insert is greatly modified by the insert itself, by the time the neutrons reach the detectors, the effect is not as prevalent as evidenced by the small difference in the doubles neutron counting rates. The signatures/observables of the Cd subtraction and Cd ratio are derived from this raw doubles data and are plotted in Fig. 14.

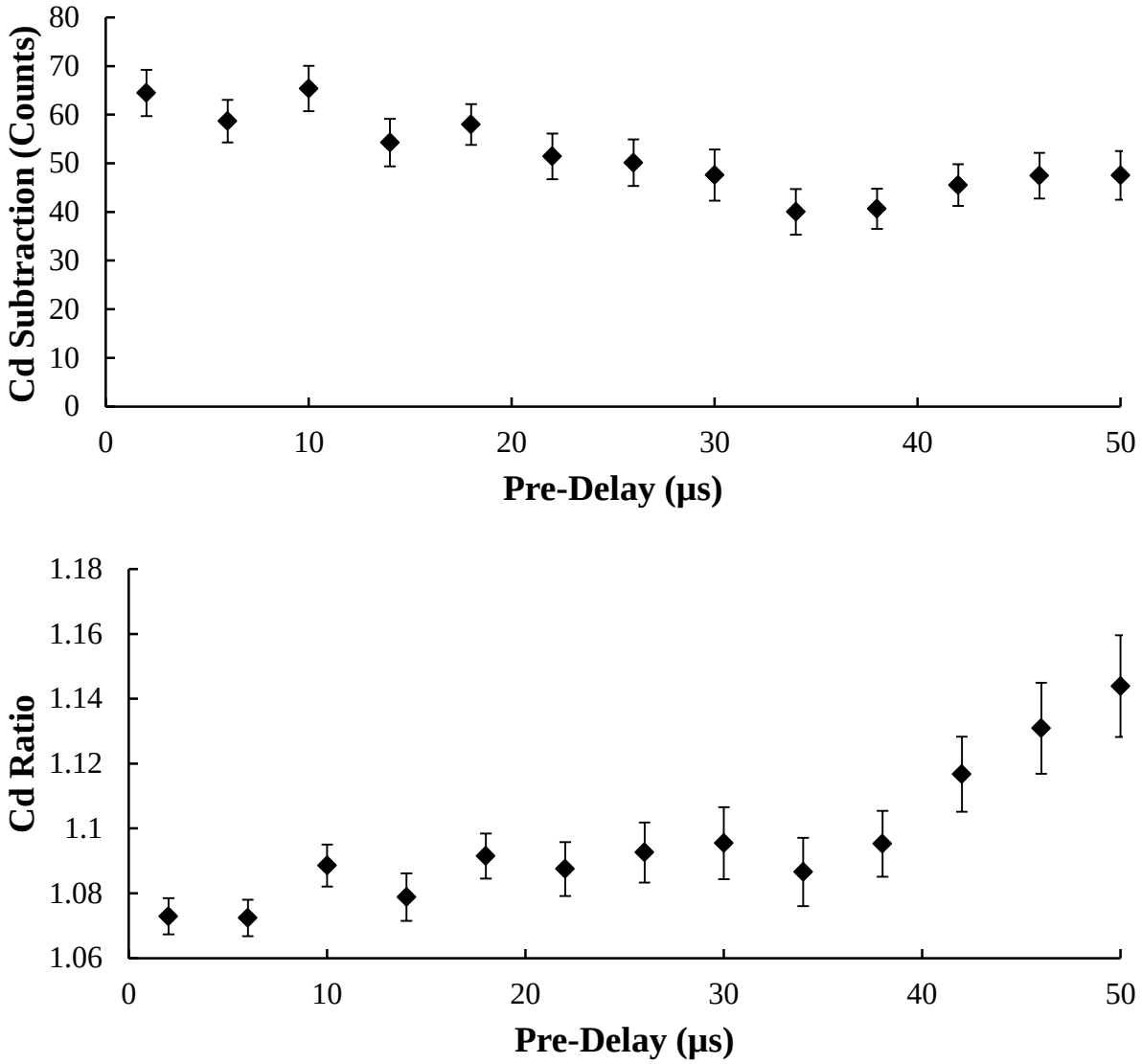

Fig. 14. Cadmium subtraction (top) and cadmium ratio (un-normalized) (bottom) as a function of pre-delay.

These signatures are derived from the primary data.

Figure 14 shows that the Cd subtraction and Cd ratio have difference time trends and are, therefore, not measures of the same physical effect. However, the two signatures do appear to share the same minimum point at 34 µs.

It can be observed from the data in Fig. 14 that the Cd subtraction appears to have two maxima, as predicted in the theory section. The Cd subtraction peaks at ~10 μs, falls to a minimum at 34 μs, and then appears to peak again at ~46 μs. It is thought that these two maxima correspond to the two fission processes that lead to multiplication within the item, drawn out by the neutron thermalization time in the counter body HDPE.

Figure 14 shows that the Cd ratio is increasing with time over the range of pre-delay settings investigated. This corresponds to a timescale of 2 μs to 54 μs from the start of the first pre-delay to the end of the last coincidence gate. Moving the gate out in time not only increases the Cd ratio but it also increases the uncertainty on the Cd ratio (likely from an increased accidentals contribution). This was the same effect seen in previous simulation work [13]. There is trade-off between finding the largest possible ratio while at the same time minimizing the accidentals (random chance coincidence) contribution to the uncertainty. This signature may be misleading because reactivity will not continue to increase with time for a sub-critical system, but instead it should peak following the interaction of the thermal neutron albedo with the item.

It would be useful future work to run the same set of measurements with ^{252}Cf only. This would reveal whether the primary fission process causes the first maximum. In turn, it would reveal the magnitude of the effect.

2.10 FINAL DATA SET—CADMIUM RATIO AND CADMIUM SUBTRACTION AS A FUNCTION OF FISSILE MASS

Final measurements were performed using the traditional inspection gate settings of a 4.5 μs pre-delay and a 64 μs gate width. All of the available uranium items were assayed with a mass range of 0.52–181 g, corresponding to a range of enrichment values between 0.31–93.17 wt% ^{235}U.

Table 7. Cd ratio and Cd subtraction values with uncertainties as a function of ^{235}U mass

^{235}U Mass (g)	Cd Ratio	σ(Cd Ratio)	Relative Uncertainty (%)	Cd Subtraction	σ(Cd Subtraction)	Relative Uncertainty (%)
0	1.008	0.002	0.167	59.1	12.5	21.1
0.52	1.012	0.002	0.164	88.7	12.2	13.8
4.99	1.031	0.002	0.165	231.5	12.4	5.4
7.54	1.038	0.002	0.159	278.3	12.0	4.3
39.1	1.068	0.002	0.148	512.5	11.6	2.3
101.72	1.093	0.002	0.152	711.0	12.2	1.7
181.15	1.099	0.002	0.167	771.9	13.7	1.8

The data in Table 7 shows that the Cd subtraction is non-zero within 3 sigma for the zero mass sample (blank can). The Cd ratio shows a 0.8% effect at zero mass. This suggests that something else is impacting these signatures as zero mass, such as an unexpected neutron background. The Cd ratio will amplify a change in efficiency between the two measurement conditions and, therefore, make a background signal appear as a real signature. The Cd subtraction will reveal doubles rates present in the background.

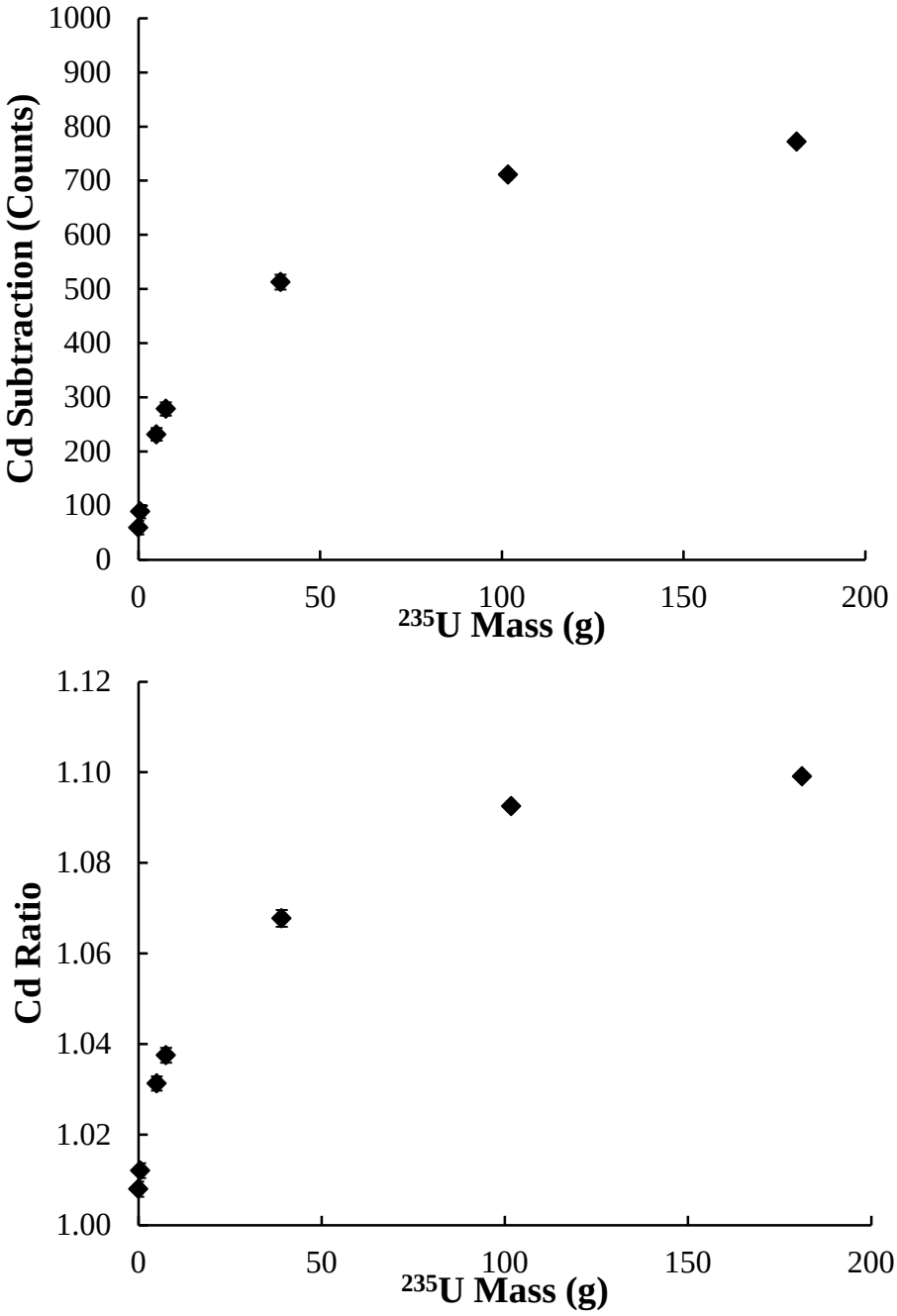

Fig. 15. Cadmium subtraction (top) and Cd ratio (bottom) as a function of fissile mass.

In this experiment, a 64 μs gate width was used, compared with the 4 μs gate width used to sample the time profile for the pre-delay setting method. It can, therefore, be observed in Fig. 15 that the y-axis is larger in magnitude, and the uncertainties in both the Cd subtraction and Cd ratio values are smaller than those observed in the pre-delay setting method for the same count time.

Based on the functional form for the Cd subtraction predicted by Eq. (14), this graph should exhibit a trend that goes by multiplication to the third power (i.e., cubic in M). However, this is not the case, and instead, a saturation effect can be observed. This saturation effect suggests that perhaps self-shielding is a more significant effect than multiplication for these small samples. The Cd subtraction is underreporting the fissile mass due to self-shielding, which means that thermal albedo neutrons are not fully penetrating the sample to induce fission uniformly within the item [18].

The graphs have the same shape, which suggests that the Cd ratio is also underreporting the fissile mass for these small samples due to self-shielding. The issue of self-shielding could be addressed in both cases by using a Cd mode interrogation, i.e., surrounding the ^{252}Cf interrogation source with Cd to achieve a predominantly fast-neutron spectrum.

In conclusion, a difference cannot be discerned between these two graphs. However, they may only look similar due to the conditions of the measurement (i.e., low multiplication, self-shielding). Visually, the graphs appear similar because the Cd subtraction is small for this sample, but the time profile distribution plots have shown that they are not the same metric.

The Cd subtraction is given by Eq. (19) below [refer to Eq. (16)]:

$$CS = D - D' \tag{19}$$

In the limit where doubles neutron counting rate and modified doubles neutron counting rate are small, the Cd ratio approximates to our functional form for the Cd subtraction:

$$CR = \frac{D}{D'} \sim \frac{D' + (D - D')}{D'} \sim 1 + \frac{(D - D')}{D} \tag{20}$$

Therefore, these signatures are measuring two different effects.

In conclusion of this final experiment, self-shielding and saturation are more significant effects than multiplication in these samples. However, the Cd subtraction shows a measurable signature. The Cd subtraction data can be fit to a calibration curve in INCC and used as a signature for fissile mass. The extent of the present experimental study was limited in scope and by item availability, but these findings under non-ideal conditions are certainly encouraging.

3. CONCLUSIONS

The thought process behind the Cadmium Subtraction Project was motivated by the fact that a number of safeguards technologies under current development are based on the use of a re-entrant neutron flux, yet the Cd ratio has not been proven to provide a direct measurement of item multiplication, i.e., it does not provide a signature that maps uniformly to multiplication. Through this project work, the theory of the Cd subtraction method has been documented and a functional dependence has been derived to guide the measurement campaign. The project provided the first preliminary experimental investigation into the use of a Cd subtraction method compared with a Cd ratio method. Experimental measurements have been used as a guide to reveal the correct approach for field implementation and to answer the following research question: *Are the predicted functional dependences evident from the measured data?* The following conclusions can be drawn from the experimental measurement campaign.

- The Cadmium Subtraction Project has demonstrated the use of the LAWCC in a new mode using ^{252}Cf as an interrogation source and a re-entrant neutron flux (thermal neutron albedo). The ability to use the LAWCC with a ^{252}Cf interrogation source has the potential to eliminate the need for AmLi sources for the active neutron interrogation of uranium (^{235}U).
- Through the project experimental measurement campaign, practical experience (setup and calibration) and insight have been gained for NDA measurements based on a thermal neutron albedo. Experience has also been gained in the acquisition and analysis of measured data based on an AANI measurement using the LAWCC.
- The Cd subtraction signature showed a measurable effect. The traditional Cd ratio signature also showed a measurable effect. It is interesting that the experiment showed statistical viability in these individual signatures with a modest neutron counter (i.e., lower efficiency than the counters typically used for this type of experiment).
- The Cd subtraction and Cd ratio each provide a signature that could be fit to a calibration curve and, therefore, are practical for the assay of uranium.
- When performing measurements based on a thermal neutron albedo, self-shielding cannot be neglected. The Cd subtraction and Cd ratio calibration curves indicate that self-shielding and saturation are more significant for these samples than multiplication. The self-shielding issue could be overcome by keeping the interrogation spectrum fast. However, this may change the mode of operation from a Cd–no Cd approach to a late–early gate approach like DDSI.
- A signature is still needed that is a direct observable of multiplication, i.e., a signature that maps uniformly to item multiplication. Under certain conditions, a Cd subtraction or difference may yield a more direct observable of multiplication that the traditional Cd ratio. However, more work needs to be done to demonstrate this since there is no obvious merit of one method over the other with this data set because the signal was small. The small signal was due to low item multiplication ($M-1 \sim$ few %) because of the small mass of fissile material. Consequently, the capabilities and limitations of the two methods could not be fully explored and tested.
- For success, higher mass (kilograms) of material are needed. Secondly, an NDA system is needed that can measure the reaction kinematics and time profile behavior of the coupled item-detection system. This may be achieved by a slight redesign of current systems (e.g., less polyethylene or a new configuration) to achieve a shorter die-away time or by fast-neutron detection based on proton recoil. The signature could be explored to a more complete extent using fast-neutron detection.

- The coincidence gate fraction changes with time after a ^{252}Cf spontaneous fission event during a measurement with a re-entrant neutron flux, which has been demonstrated in the pre-delay experiment.
- The change in the coincidence gate fraction with time must be taken in to account when determining the optimal coincidence gating structure (pre-delay and coincidence gate width), which is a concept that was first explained by Evans et al. [17].
- It has been found that the physics of the instrument response and the kinematics of the reaction processes within the coupled item-detection system are often hidden by routine calibration procedure and traditional settings. Current neutron counter settings (4.5 μs pre-delay and 64 μs gate width) were designed for use based on the HLNCC-II decades ago. It is time to rethink some of the traditional approaches to measurement using neutron well counters. The same instruments can be used, but incremental R&D could be performed to investigate the optimum settings. This could yield more direct observables for quantities of interest.
- The potential merit of using an alternative procedure for setting the pre-delay and determining the coincidence gate fractions has been demonstrated. However, the statistics in the time profile study were not good enough to discern the time trend of these signatures.
- Some lessons were learned for field implementation for signatures (e.g., Cd subtraction and Cd ratio) derived from the primary measured data/observables (e.g., doubles neutron counting rate). When operating an instrument based on derived signatures, counting times should be optimized based on these signatures and not the individual neutron counting rates. In simulation design studies, this point is often neglected because the impact of accidentals is not predicted by the MCNPx code and is, therefore, often not propagated through the uncertainty to determine the optimum count time. However, it is relatively straightforward to simulate the accidentals by post-processing the results of MCNPx. For example, pulse train simulation work is being performed at LANL under a separate NA-22 project.
- Also relevant to field implementation, although not investigated here, measurements performed underwater (e.g., spent nuclear fuel measurements) vs. measurements performed in air will observe a different instrument response.

These findings emphasize the need for incremental R&D for safeguards technology. NDA instruments themselves do not always have to be redesigned or completely reimagined to generate new methods or new signatures/observables, or indeed to optimize current signatures/observables. The experimental findings illustrate that a reliance on traditional IAEA settings for coincidence counting (4.5 μs pre-delay and 64 μs gate width) and the procedures used to derive those settings should be challenged and reconsidered when the measurement objective is to derive signatures other than the doubles rate, especially when the counter time behavior is varying due to a re-entrant neutron flux. It is not always necessary to redesign new hardware or create transformational techniques to extract new signatures from current NDA methods and to yield new ways to observe fissile content. As this project has demonstrated, incremental R&D such a changing the coincidence gate settings, or delaying a coincidence gate in time, can vary and in turn improve the signature. Future work on signature optimization is recommended in the next section of the report. In particular, active interrogation is of interest for uranium assay and exploiting spectral shape is a relatively unexplored possibility.

4. RECOMMENDATIONS FOR FUTURE SAFEGUARDS TECHNOLOGY DEVELOPMENT WORK

The following items are recommended for future safeguards technology development efforts:

- High-fidelity simulations would offer a short-term gain in terms of understanding the time profile and comparing it for items of different masses.
- Phased experiments are recommended using the LAWCC with the insert already developed for this project.
    - Firstly, it would be valuable to simply repeat the time profile experiment for the highest mass item with longer counting times.
    - Secondly, the counter could be operated in fast interrogation mode (with Cd). A calibration curve could then be determined for ^{235}U mass using the optimal gating structure and with a reduced self-shielding effect. However, this second experiment would require a DDSI-type late–early gate interpretation rather than a Cd–no Cd mode.
    - Thirdly, a ^{252}Cf-only measurement could be performed for comparison and for more detailed characterization of the ^{252}Cf time profile.
    - Finally, ring ratios (using the front and back ring of ^{3}He tubes) could also be used to empirically discern both energy and efficiency differences during the two measurement conditions (Cd and no Cd). Ring ratios are fairly standard for waste matrix corrections but are not commonly applied to safeguards neutron counting. The ring ratio method assumes that there are viable statistics on the doubles neutron counting rate in a single ring, which would have to be investigated.
- A list mode board is now available at ORNL and could be leveraged for incremental R&D now that this active neutron interrogation experiment has been set up and is also readily available. In turn, the list mode experiments could be used in conjunction with simulation experiments to better understand the changes in gate fraction for this type of experiment. The results from R&D into the optimal procedures for gate setting and signature acquisition could be distilled to a useable procedure for IAEA inspectors in the field.
    - The temporal studies (e.g., Sect. 2.9) would be more effectively performed using list mode electronics. List mode would enable a wider range of pre-delay settings to be explored within a single (long) count.
- The IAEA has verbally expressed interest in fast-neutron counting methods for safeguards detection, the use of which may enable the signature to be resolved. This project could be linked to fast-neutron imaging systems based on PSD plastics [18]. Measurements could be performed to understand whether there is merit to extending that technique with the use of a ^{252}Cf interrogation source and uranium measurements performed in the Cd and no Cd modes.
- Existing data from the PNAR-FC and PNEM instruments could be analyzed using a Cd subtraction approach by their respective developers at LANL in collaboration with ORNL. However, PNEM is the only one of these two experiments that employs the doubles neutron counting rate.
- Bulk quantities of uranium oxide and metal could be measured and simulated.
- Self-shielding studies performed over the range DU–5 wt% ^{235}U [19], where DU is depleted uranium, could be extended over a greater range of enrichments. This impacts applied calibration.

Longer-term R&D efforts would include:

  - Experimentally, we observe six signatures: the singles, doubles, and triples neutron counting rates with and without Cd. Gate fractions can be determined during calibration. However, the optimal combination of all these signatures should be determined for all relevant NDA techniques, mapped against attributes of interest.
- The point model approach could be extended to measurement situations with a returning albedo neutron flux (energy-dependent point model).
- A two-component, two-energy group approximation is needed to fully describe the physics of this measurement scenario. Directional flux tallies could be employed to determine how many neutrons cross each boundary of the items of interest and the reflector, and what percentage of the source neutrons reenter the sample [11]. This would need to be combined with a fission rate tally. Furthermore, flux vs. energy-group tallies could be used to create importance maps.

5. REFERENCES

1. H.O. Menlove and D.H. Beddingfield, *Passive Neutron Reactivity Measurement Technique*, LA-UR-97-2651, May, 1997.
2. R.D. McElroy Jr., S. Croft, and S.L. Cleveland, "Preliminary Performance Results for a Direct Multiplication Measurement for Use in Neutron Multiplicity Analysis," in Proceedings of the Institute of Nuclear Materials Management (INMM) 55th Annual Meeting, July (2014).
3. J.L. Conlin and S.J. Tobin, *Predicting Fissile Content of Spent Nuclear Fuel Assemblies with the Passive Neutron Albedo Reactivity Technique and Monte Carlo Code Emulation*, LA-UR-10-06933, 2010.
4. L.G. Evans, S.J. Tobin, M.A. Schear, S. Croft, M.T. Swinhoe, and H.O. Menlove, *Report on the Performance of Passive Neutron Albedo Reactivity with Helium-3 Tubes (PNAR-^{3}He): For the Non-Destructive Assay (NDA) of Spent Nuclear Fuel*, Los Alamos National Laboratory Report, 2010.
5. K.A. Miller, H.O. Menlove, M.T. Swinhoe, and J.B. Marlow, *A New Technique for Uranium Cylinder Assay Using Passive Neutron Self-Interrogation*, IAEA-CN-184/131.
6. A.C. Kaplan, V. Henzl, A.P. Belian, M.T. Swinhoe, M. Flaska, and S.A. Pozzi, "Total Plutonium Content Determination in Pressurized-Water Reactor Spent Fuel with the Differential Die-Away Self-Interrogation Instrument," in Proceedings of the Institute of Nuclear Materials Management (INMM) 55th Annual Meeting, July (2014).
7. H.O. Menlove, S.H. Menlove, and S.J. Tobin, *Verification of Plutonium Content in Spent Fuel Assemblies Using Neutron Self-Interrogation*, LA-UR-08-07479.
8. S.J. Tobin, W.S. Charlton, M.H. Ehinger, M.L. Fensin, A.S. Hoover, H.O. Menlove, B.J. Quiter, A. Rajasingam, N.P. Sandoval, S.F. Saavedra, D. Strohmeyer, M.T. Swinhoe, and S.J. Thompson, "Determining plutonium in spent fuel with nondestructive assay techniques," in Proceedings of the 31st Annual Meeting of ESARDA, May 26-28, (2009), Vilnius, Lithuania.
9. A.M. Bolind, "Development of an analytical theory to describe the PNAR and CIPN nondestructive assay techniques," *Annals of Nuclear Energy*, **66**, 167–176 (2014).
10. L.G. Evans, S.J. Tobin, S. Croft, and M.A. Schear, *Gate width optimization for Passive Neutron Albedo Reactivity (PNAR)*, ANS (2010).
11. L.C.-A. Bourva, S. Croft, and D.R. Weaver, "The effect of albedo neutrons on the neutron multiplication of small plutonium oxide samples in a PNCC chamber," *Nuclear Instruments and Methods in Physics Research A*, **479**, 640–655 (2002).
12. A.M. LaFleur, S-K. Ahn, H.O. Menlove, M.C. Browne, and H-D. Kim, "Characterization and performance evaluation of a new passive neutron albedo reactivity counter for safeguards measurements," *Radiation Measurements*, **61**, 83–93 (2014).
13. D.M. Cifarelli and W. Hage, "Models for a three-parameter analysis of neutron signal correlation measurements for fissile material assay," *Nuclear Instruments and Methods in Physics Research A*, **251**, 550–563 (1986).
14. N. Ensslin, W.C. Harker, M.S. Krick, D.G. Langner, M.M. Pickrell, and J.E. Stewart, *Application Guide to Neutron Multiplicity Counting*, LA-13422-M.
15. *INCC Software User's Manual*, Los Alamos National Laboratory, November 1, 2005.
16. R.D. McElroy, Jr., *Neutron Multiplicity Analysis*, Canberra Training Course, June, 2006.
17. L.G. Evans, M.A. Schear, S. Croft, S.J. Tobin, M.T. Swinhoe, and H.O. Menlove, "Non-destructive Assay of Spent Nuclear Fuel using Passive Neutron Albedo Reactivity," in Proceedings of the Institute of Nuclear Materials Management (INMM) 51st Annual Meeting, July (2010).
18. J. Newby, P. Hausladen, and M. Blackston, "Position-Sensitive Organic Scintillation Detectors for Nuclear Material Accountancy", in Proceedings of the IAEA Symposium on International Safeguards, October (2014).

19. S. Croft, E. Alvarez, R.D. McElroy, and C.G. Wilkins, “The Absolute Calibration of Active Neutron Assay Instruments,” in Proceedings of the 27th Annual ESARDA Symposium, London, England, May 2005. EUR 21674 EN (2005) Paper P080, ISBN 92-894-9626-6.